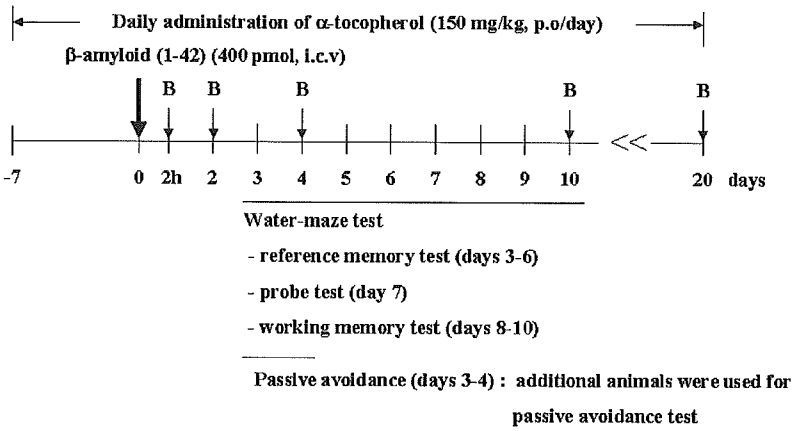

Fig. 1. Experimental schedule. B: biochemical measurements (enzyme activity, lipid peroxidation, and protein oxidation).

2.3.1. Reference memory test

For each training trial, the mouse was put into the pool at one of the five positions, the sequence of the positions being selected randomly. The platform was located a constant position throughout the test period in the middle of one quadrant, equidistant from the center and edge of the pool. In each training session, the latency to escape on to the hidden platform was recorded. If the mouse found the platform, it was allowed to remain there for 10 s and was then returned to its home cage. If the mouse was unable to find the platform within 60 s, the training was terminated and a maximum score of 60 s was assigned. Training was conducted for four consecutive days, four times a day, from day 3 to 6 after the start of Aβ i.c.v. injection.

2.3.2. Probe test

On day 7 after the start of Aβ i.c.v. injection, a single probe trial was conducted. The platform was removed from the pool and each mouse was allowed to swim for 60 s in the maze. The number of times the mouse crossed the annulus where the platform had been located was recorded.

2.3.3. Working memory (repeated acquisition) test

Working memory test was conducted three consecutive days from day 8 to 10 and consisted of five trials per day. The working memory test was procedurally similar to reference memory test except that the platform location was changed daily. The first trial of the day was an informative sample trial in which the mouse was allowed to swim to the platform in its new location. Spatial working memory was regarded as the mean escape latency of the second to fifth trials.

2.4. Passive avoidance test

Passive avoidance was measured using a Gemini Avoidance System (San Diego Instrument, San Diego, CA) which consists of two-compartment shuttle chambers with a constant current shock generator. On an acquisition trial, each mouse was placed into the start chamber, which remained darkened. After 20 s, the chamber light was illuminated and the door was opened for mouse to move into the dark chamber freely. Immediately it entered the dark chamber, the door was closed and an inescapable scrambled electric shock (0.3 mA, 3 s, once) was delivered through the floor grid. Then the mouse was returned to its home cage. Twenty-four hours later, each mouse was again placed in the start chamber again (retention trial). The interval between the placement in the lighted chamber and the entry into the dark chamber was measured as latency in both acquisition and retention trials (maximum 300 s) [51,52].

2.5. Tissue preparation

Mice were anesthetized with pentobarbital (50 mg/kg) and then perfused transcardially with ice-cold 0.9% NaCl (10 ml/10 g body weight) to remove the free radical-scavenging and -generating sources in the brain [23]. The cerebral cortex, hippocampus were carefully excised, and the tissues stored at −70 °C. Homogenates were sonicated for 30 s in a cell disruptor (Bronson Sonic, NY) and centrifuged at 10,000 × *g* for 20 min. The resulting supernatant was used to measure activities of glutathione peroxidase (GPX) and glutathione reductase (GRX).

2.6. Determination of superoxide dismutase (SOD)

Homogenates of hippocampus or cerebral cortex were centrifuged at 25,000 × *g* for 15 min at 4 °C and supernatant dialyzed in 50 mM PBS (pH 7.8) containing 1 mM EDTA. SOD activity was determined based on inhibition of superoxide-dependent reactions. The reaction mixture contained 70 mM potassium phosphate buffer (pH 7.8), 30 μM cytochrome *c*, 150 μM xanthine, and tissue extract in phosphate buffer diluted 10 times with PBS in a final volume of

3 ml. The reaction was initiated by adding 10 μl of 50 units xanthine oxidase, and the change in absorbance at 550 nm recorded. One unit of SOD is defined as the quantity required to inhibit the rate of cytochrome *c* reduction by 50%. For estimating total SOD, 10 μM potassium cyanide (KCN) was added to the medium to inhibit cytochrome oxidase activity [32]. For estimating Mn-SOD activity, 1 mM KCN was added to the incubation mixture to inhibit Cu,Zn-SOD activity [32]. The activity of Cu,Zn-SOD was calculated by the subtraction of the Mn-SOD activity from the total SOD activity.

2.7. Determination of glutathione peroxidase (GPX)

GPX activities of the hippocampus and cortex were analyzed by a spectrophotometric assay described by Lawrence and Burk [27], using 2.0 mM reduced glutathione and 0.25 mM H_2O_2 as substrate. One unit of GPX is defined as the quantity that catalyzes the oxidation of 1 nM NADPH/min at 25 °C. Protein was measured using the BCA protein assay reagent and bovine serum albumin was used as a standard.

2.8. Determination of glutathione reductase (GRX)

GRX activities were measured based on the method discribed by Eklow et al. [13]. The reaction mixture contained 1 mM oxidized glutathione and 100 μl of sample in phosphate buffer (pH, 7.0) containing 1 mM EDTA. The reaction started with adding NADPH (final concentration of 0.11 mM) and the decrease in absorbance of NADPH at 340 nm was measured. One unit of activity is defined as 1 nM of NADPH oxidized.

2.9. Determination of malondialdehyde (MDA)

The amount of MDA in homogenates of hippocampus, cerebral cortex was determined by the methods of Jareno et al. [20] with some modification [22,23]. In brief, 0.1 ml of the homogenate diluted 10 times with phosphate buffered saline (PBS) was mixed with 0.75 ml working solution (thiobarbituric acid 0.37% and perchloric acid 6.4%, 2:1, v/v) and heated to 95 °C for 1 h. After cooling (10 min in ice water bath), the flocculent precipitate was removed by centrifugation at 3200 × *g* for 10 min. The supernatant was neutralized and filtered prior to injection on a octadecylsilane 5 μm column. Mobile phase consisted of 50 mM PBS (pH 6.0):methanol (58:42, v/v). Isocratic separation with 1.0 ml/min flow rate and detection at 532 nm using a UV–vis high-performance liquid chromatography detector were performed.

2.10. Determination of protein carbonyl

The extent of protein oxidation in the cerebral cortex and hippocampus was assessed by measuring the content of protein carbonyl groups, which was determined spectrophotometrically with the 2,4-dinitrophenylhydrazine (DNPH)-labeling procedure as described by Oliver et al. [41]. The results are expressed as nmol of DNPH incorporated/mg protein [23] based on the extinction coefficient for aliphatic hydrazones of 21 mM^{-1} cm^{-1}. Protein was measured using the BCA protein assay reagent (Pierce, Rockford, IL, USA).

2.11. Statistics

Data are expressed as the mean ± S.E.M. The statistical significance in the behavioral and biochemical effects of α-tocopherol was determined by one-way analysis of variance (ANOVA), followed by Bonferroni's test or ANOVA with Duncan's new multiple (DMR) test. Two-way ANOVA was conducted to analyze data from water maze training trials.

3. Results

3.1. Effects of α-tocopherol on performance of the water maze task by Aβ (1–42)-treated mice

The changes in escape latency onto a hidden platform produced by training trials are shown in Fig. 2A. Two-way ANOVA with all treatment groups showed significant effects mainly of group ($F_{3576} = 9.084$, $P = 6.97 \times 10^{-6}$) and training ($F_{15,576} = 13.772$, $P = 4.82 \times 10^{-30}$), but not group by trial interactions ($F_{45,576} = 0.449311$, $P = 1.00$). The escape latencies of Aβ(1–42)-injected mice were significantly delayed, as compared to those of Aβ(40–1)-injected mice ($P < 0.0005$; post-hoc analysis). Prolonged treatment with α-tocopherol significantly improved the Aβ(1–42)-induced impairment of performance ($P < 0.05$; post-hoc analysis).

The results of the 60 s probe test also showed significant memory impairment in the Aβ (1–42)-treated mice. The number of annulus crossings, representing the number of passes over the platform site, was significantly decreased ($F_{118} = 5.40$, $P = 0.032$) in the Aβ (1–42)-treated mice as compared to Aβ (40–1)-treated mice. This was significantly reversed ($F_{118} = 6.08$, $P = 0.024$) by α-tocopherol administration (one-way ANOVA) (Fig. 2B).

Working memory was assessed as the mean escape latency of the second to the fifth trials (test trials), for three days. There were no significant differences among the four groups in the sample trials (the first trial) of three consecutive days (data not shown). However, the mean escape latency during test trials of the Aβ (1–42)-treated mice was significantly longer ($F_{1238} = 5.06$, $P = 0.026$) than that of the Aβ(40–1)-treated mice. Repeated treatment with α-tocopherol significantly ameliorated ($F_{1238} = 4.13$, $P = 0.043$) the Aβ(1–42)-induced impairment of performance in working memory test (one-way ANOVA). There was no significant difference between Aβ(40–1)-treated mice and α-tocopherol- plus Aβ(40–1)-treated mice in the hidden platform test, probe, or working memory tests (Fig. 2C).

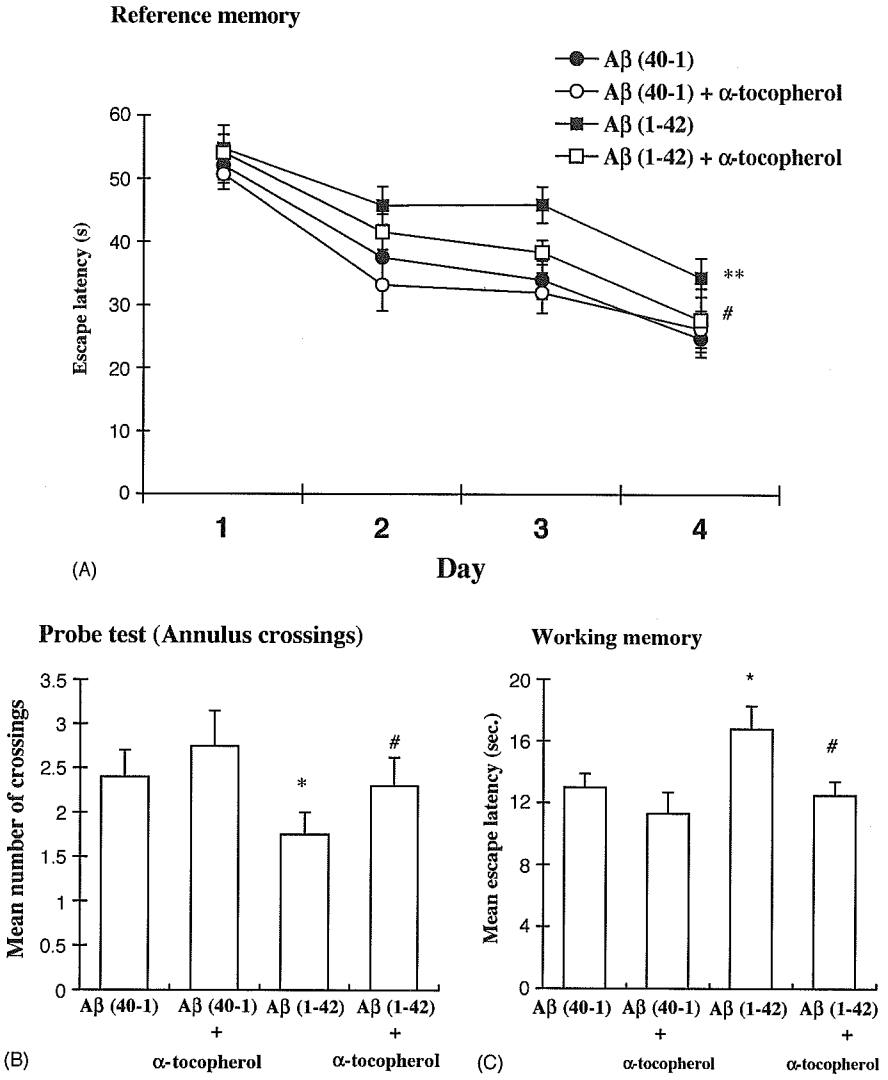

Fig. 2. The effects of α-tocopherol on the performance of Aβ (1–42)-treated mice in the training (A), probe trial (B), and working memory (C) trials of the water maze test. The training trials were carried out on days 3–6 (four per day), the probe trials were performed on day 7, and the working memory trials (five per day) were carried out on days 8–10 after the i.c.v. injection of Aβ. Each value is the mean ± 10 animals. The statistical significance of the training trials was calculated using two-way ANOVA followed by post-hoc analysis, and those of the probe and working memory trials were calculated using one-way ANOVA. $^{*}P < 0.05$ or $^{**}P < 0.0005$ vs. Aβ (40–1)-treated mice, $^{\#}P < 0.05$ vs. Aβ (1–42)-treated mice.

3.2. Effects of α-tocopherol on performance of the passive avoidance task by Aβ(1–42)-treated mice

In the acquisition trial, the step-through latencies did not differ among the four groups. The step-through latency in the retention trial was significantly decreased ($F_{118} = 19.79$, $P = 0.00031$) in the Aβ(1–42)-treated mice, as compared to the Aβ(40–1)-treated mice. The α-tocopherol-plus Aβ(1–42)-treated mice showed a significantly longer step-through latency ($F_{118} = 4.65$, $P = 0.045$) than did the Aβ(1–42)-treated mice. There were no significant differences between the Aβ(40–1)-treated and α-tocopherol- plus Aβ (40–1)-treated mice in the acquisition trial or retention trials (Fig. 3).

3.3. Effects of α-tocopherol on Cu,Zn-SOD activity in the brains of Aβ (1–42)-treated mice

Cu,Zn-SOD activity did not significantly change in the absence of Aβ (1–42). However, Aβ (1–42) treatment resulted in early increases in Cu,Zn-SOD activity in the cerebral cortex and hippocampus [at 2 h and 2 days: $P < 0.01$ versus Aβ (40–1); at 4 days: $P < 0.05$ versus Aβ (40–1)]. The enzyme activity in the cerebral cortex was comparable

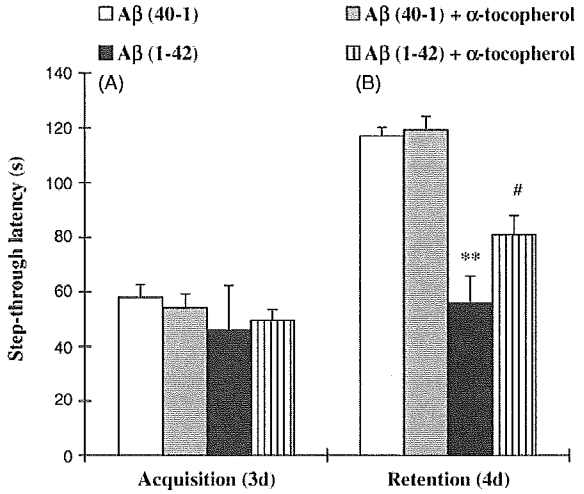

Fig. 3. The effects of α-tocopherol on the performance of Aβ (1–42)-treated mice in the acquisition (A) and retention (B) trials of the passive avoidance task. The task was performed on days 3–4 after the i.c.v. injection of Aβ. Each value is the mean ± 10 animals. $^{**}P < 0.0005$ vs. Aβ (40–1)-treated mice, $^{\#}P < 0.05$ vs. Aβ (1–42)-treated mice (one-way ANOVA).

to that in the hippocampus. Increases in Cu,Zn-SOD activity induced by Aβ (1–42) were significantly attenuated in the presence of α-tocopherol [at 2 h and 2 days: Aβ (1–42) versus Aβ (1–42) plus α-tocopherol, $P < 0.05$]. Increases in Cu,Zn-SOD activity had returned to near vehicle or Aβ (40–1) levels at 10 days (Fig. 4A).

3.4. Effects of α-tocopherol on Mn-SOD activity in the brains of Aβ (1–42)-treated mice

The animals treated with non-toxic Aβ (40–1) or vehicle did not significantly induce Mn-SOD. Similar to Cu,Zn-SOD activity, Mn-SOD activity was significantly induced in the cerebral cortex and hippocampus with Aβ (1–42) treatment [at 2 h and 2 days: $P < 0.05$ versus Aβ (40–1)]. The enzyme activity in the hippocampus appeared to be more susceptible than the cerebral cortex activity to Aβ (1–42). The Aβ (1–42)-caused increases in Mn-SOD activity were significantly prevented by prolonged treatment with α-tocopherol [at 2 h and 2 days (both brain regions): Aβ (1–42) versus Aβ (1–42) plus α-tocopherol, $P < 0.05$]. The increases in Mn-SOD activity had returned to near vehicle or Aβ (40–1) levels at 4 days (Fig. 4 B).

3.5. Effects of α-tocopherol on GPX activity in the brains of Aβ (1–42)-treated mice

The GPX activity did not change without Aβ (1–42) treatment. However, GPX activity was significantly increased in the cerebral cortex and hippocampus at 2 h and 2 days after i.c.v. injection of Aβ (1–42) [at 2 h and 2 days: $P < 0.05$ versus Aβ (40–1)]. Interestingly, GPX activities were also significantly induced in animals treated with Aβ (1–42) plus α-tocopherol [at 2 h and 2 days: Aβ (40–1) plus α-tocopherol versus Aβ (1–42) plus α-tocopherol, $P < 0.05$]. The GPX activity in animals treated with Aβ (1–42) was comparable to that in animals treated with Aβ (1–42) plus α-tocopherol, suggesting that α-tocopherol induced the compensative induction of GPX. No significant changes in GPX activity were observed in the cerebral cortex and hippocampus after 4 days (Fig. 5A).

3.6. Effects of α-tocopherol on GRX activity in the brains of Aβ (1–42)-treated mice

GRX activity was not apparently induced without exposure to Aβ (1–42). However, GRX activity was significantly increased at the very early stage (2 h) post-Aβ(1–42) insult [at 2 h: $P < 0.05$ versus Aβ (40–1)]. Similar to GPX, GRX activity was significantly induced in the animals treated with Aβ (1–42) plus α-tocopherol [at 2 h: Aβ (40–1) plus α-tocopherol versus Aβ (1–42) plus α-tocopherol, $P < 0.05$]. The GRX activity of animals treated with Aβ (1–42) is comparable to that of animals treated with Aβ (1–42) plus α-tocopherol. The increases in GRX activity had almost returned to vehicle or Aβ (40–1) levels in the cerebral cortex and hippocampus at 2 days (Fig. 5B).

3.7. Effects of α-tocopherol on lipid peroxidation levels in the brains of Aβ (1–42)-treated mice

No differences in the lipid peroxidation levels (as MDA) were observed in the cerebral cortex or hippocampus of vehicle- and Aβ(40–1)-treated animals. Aβ(1–42)-induced increases in MDA levels still evident at 10 days [in the cerebral cortex at 2 h, 2, 4, and 10 days; $P < 0.01$, $P < 0.05$, $P < 0.05$, and $P < 0.05$ versus Aβ(40–1); in the hippocampus at 2 h, 2, 4, and 10 days; $P < 0.01$, $P < 0.01$, $P < 0.05$ and $P < 0.05$ versus Aβ(40–1)]. These increases in MDA levels were significantly attenuated by the treatment with α-tocopherol [at 2, 4, and 10 days in the cerebral cortex and hippocampus: Aβ (1–42) versus Aβ (1–42) plus α-tocopherol, $P < 0.05$]. MDA values had almost returned to those of vehicle or Aβ(40–1) levels at 20 days after Aβ(1–42) injection (Fig. 6A).

3.8. Effects of α-tocopherol on protein oxidation levels in the brains of Aβ (1–42)-treated mice

No significant changes in protein carbonyl were found in the vehicle- and Aβ(40–1)-treated animals. Similar to the MDA time course, the Aβ(1–42)-induced increases in the formation of protein carbonyl lasted for at least 10 d [in the cerebral cortex at 2 h, 2, 4, and 10 days; $P < 0.01$, $P < 0.01$, $P < 0.05$ and $P < 0.05$ versus Aβ(40–1); in the hippocampus at 2 h, 2, 4, and 10 days; $P < 0.01$, $P < 0.05$, $P < 0.05$ and $P < 0.05$ versus Aβ(40–1)]. This significant formation of

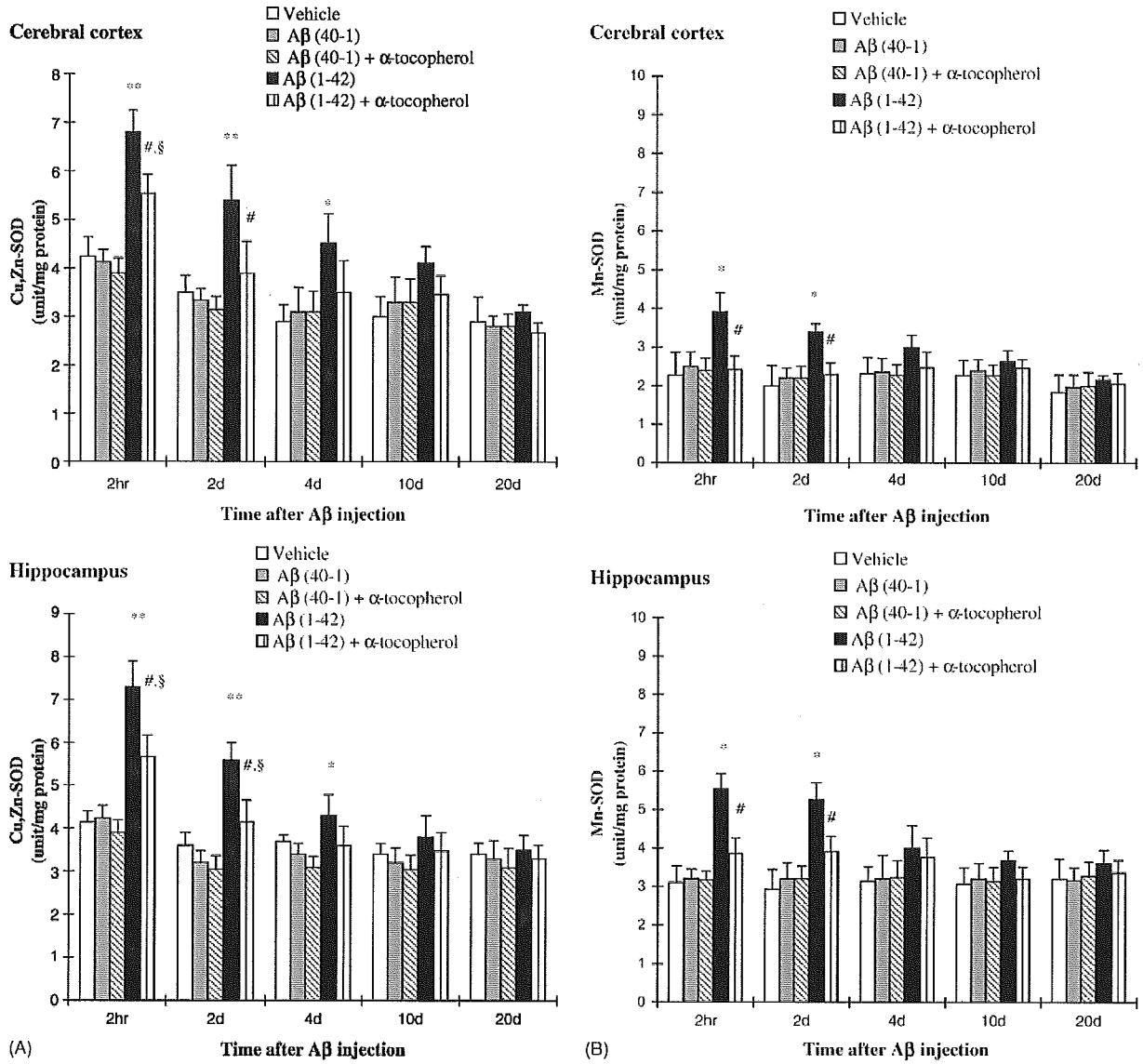

Fig. 4. The effects of α-tocopherol on the activity changes of Cu,Zn-SOD (A) and Mn-SOD (B) induced by Aβ in the cerebral cortex and hippocampus of the mice. Each value is the mean ± S.E.M. of 10 animals. $^{*}P < 0.05$ or $^{**}P < 0.01$ vs. Aβ (40–1), $^{\#}P < 0.05$ vs. Aβ (1–42), $^{\S}P < 0.05$ vs. Aβ(40–1) + α-tocopherol (ANOVA with DMR test).

protein carbonyl was significantly inhibited by the chronic treatment with α-tocopherol [at 2 h, 2, 4, and 10 days in the cerebral cortex and hippocampus: Aβ (1–42) versus Aβ (1–42) plus α-tocopherol, $P < 0.05$]. These protein carbonyl levels had returned to near basal values at 20 days after Aβ(1–42) injection (Fig. 6B).

4. Discussion

In the present study, we demonstrated that a single i.c.v. injection of Aβ (1–42) impaired performance in a water maze task and the retention of long-term memory in a passive avoidance task, in accordance with previous investigations using mice [52] and rats [39,40,51]. Similarly, acute i.c.v. injection of Aβ (25–35) in mice has also been reported to impair spatial reference memory in a water maze task [36]. These results suggest that the accumulation of neurotoxic Aβ fragments, such as Aβ (1–42) and Aβ (25–35), impairs spatial reference memory in mice, although nontoxic Aβ fragment Aβ (40–1) has no effect. Furthermore, the potent antioxidant α-tocopherol also attenuated these memory impairments (resulting in impaired performance in the passive avoidance and water maze tests) induced in mice

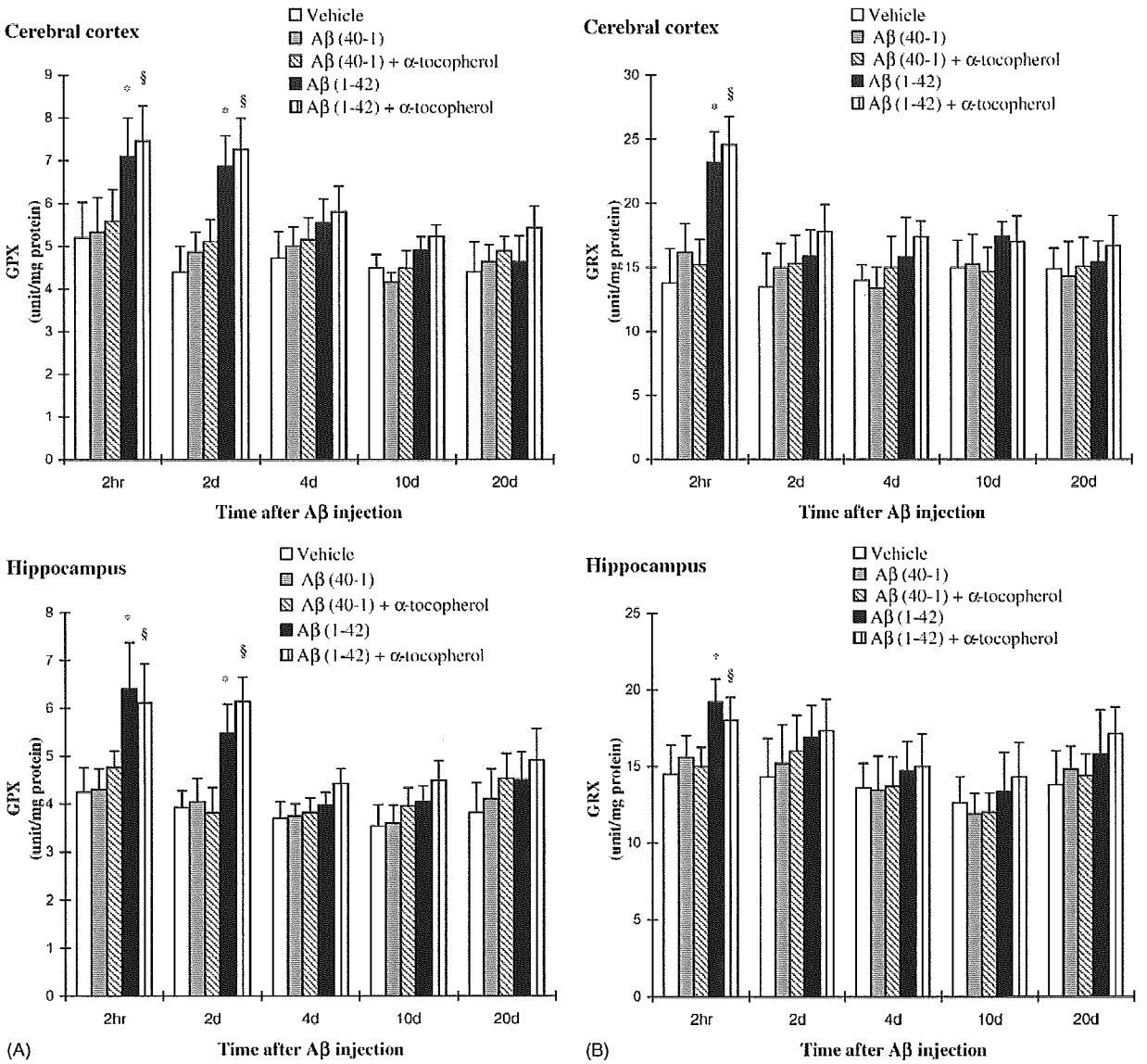

Fig. 5. The effects of α-tocopherol on the activity changes of GPX (A) and GRX (B) induced by Aβ in the cerebral cortex and hippocampus of the mice. Each value is the mean ± S.E.M. of 10 animals. $^{*}P < 0.05$ vs. Aβ (40–1), $^{\S}P < 0.05$ vs. Aβ(40–1) + α-tocopherol (ANOVA with DMR test).

by the single i.c.v. injection of Aβ (1–42). This result supports previous finding, demonstrated by Yamada et al. [51], that α-tocopherol and another antioxidant, idebenone, prevent behavioral deficits in water maze task performance in Aβ (1–42)-infused rats. However, Yamada et al. [51] did not observe increased formation of malondialdehyde (MDA) in the cerebral cortex and hippocampus of the Aβ (1–42)-infused rats at day 19 after the start of Aβ (1–42)-infusion. Similarly, we could not find a significantly increased level of MDA in mice at day 20 after a single injection with Aβ (1–42) in this study, although the levels of MDA and protein carbonyl in the cerebral cortex and hippocampus remained elevated for 10 days.

Recently, we demonstrated that continuous i.c.v. infusion of Aβ (1–42) in rats resulted in a significant decrease of the protein expressions of Mn-SOD, GSH, GPX and glutathione-*S*-transferase-π in the rat brain, suggesting that Aβ (1–42) impairs antioxidant capacity [25]. This finding indicates the cytological effects of oxidative stress induced by Aβ (1–42). In certain antioxidant systems, there might be a time lag between the synthesis of protein and the expression of mRNA following neurotoxicity

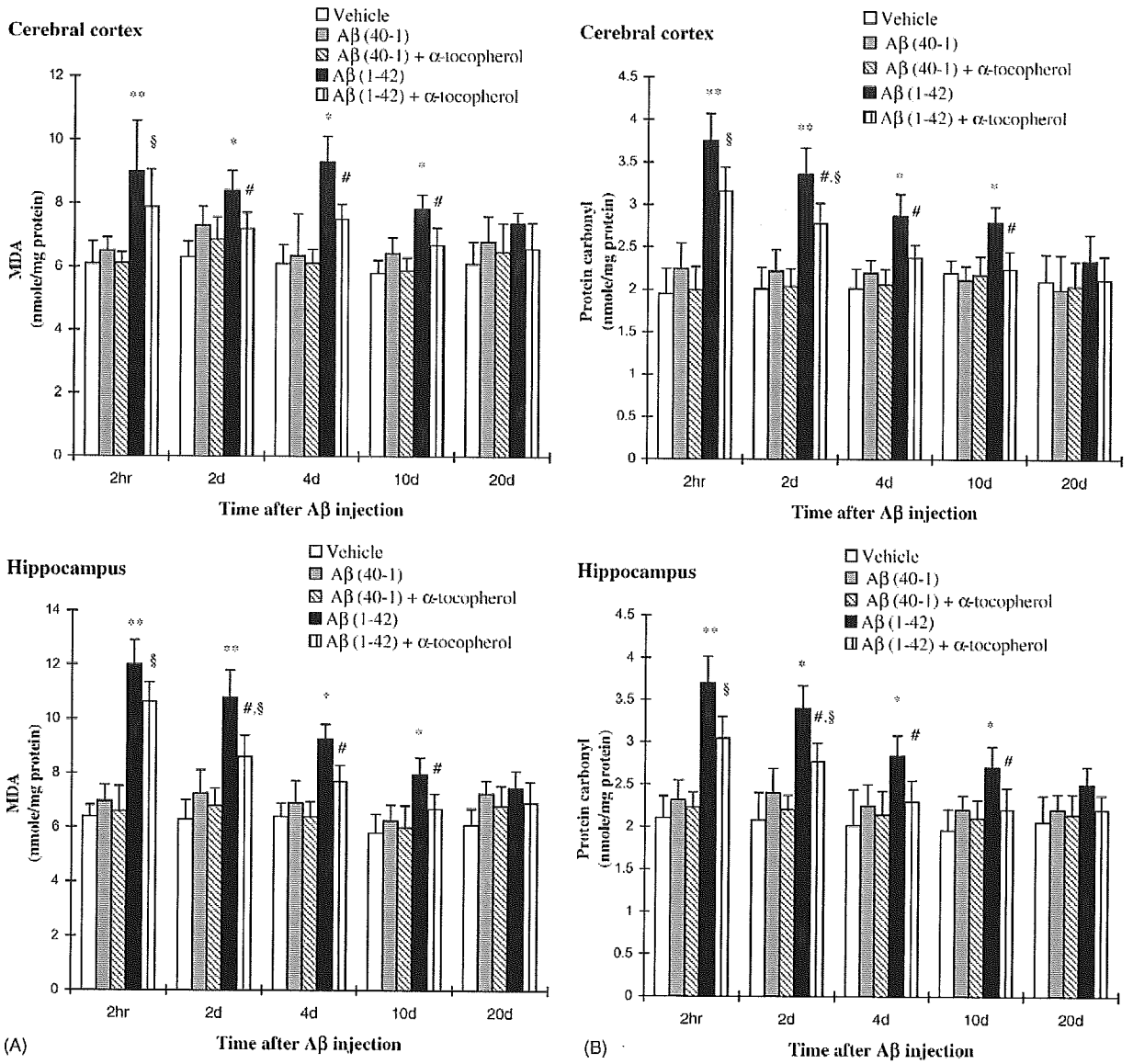

Fig. 6. The effects of α-tocopherol on the formation changes of MDA (A) and protein carbonyl (B) induced by Aβ in the cerebral cortex and hippocampus of the mice. Each value is the mean ± S.E.M. of 10 animals. $^{*}P < 0.05$ or $^{**}P < 0.01$ vs. Aβ (40–1), $^{\#}P < 0.05$ vs. Aβ (1–42), $^{\S}P < 0.05$ vs. Aβ(40–1) + α-tocopherol (ANOVA with DMR test).

[1,24]. Therefore, measurements of the activity time course of antioxidant enzymes are important when comparing the alterations induced by Aβ with those found in AD patients.

We observed significant induction of Cu,Zn-SOD, Mn-SOD, GPX and GRX activities in the cerebral cortex and hippocampus of the Aβ (1–42)-treated mice, although these changes were not observed in Aβ (40–1)-treated mice. To our knowledge, this is the first time that Aβ-induced increases of the activity of overall antioxidant enzymes have been described in the brain of an animal model. The increases in the activity of Cu,Zn-SOD were the most pronounced among these enzymatic antioxidants. The elevation in Cu,Zn-SOD activity appeared to parallel increases in MDA and protein carbonyl in the same areas, suggesting that these events are needed to scavenge superoxide radicals induced by Aβ (1–42).

The present findings support the hypothesis that increased Cu,Zn-SOD activity can lead to an accumulation of H_2O_2, which, in the absence of a simultaneous increase in GPX activity, could increase the Fenton reaction, leading to the stimulation of lipid peroxidation and protein oxidation resulting,

in cellular damage [6,11,22]. Furthermore, an uncompensated excess of Cu,Zn-SOD may contribute to the loss of neurons in selective areas in AD. This idea is supported by the fact that Down's syndrome, which includes a triplication of the Cu, Zn SOD gene and correspondingly increased enzyme activity, invariably involves degenerative changes similar to Alzheimer's disease [8]. Overall, these findings suggest that Cu,Zn SOD may play a role in Alzheimer's pathology.

Extensive evidence exists for lipid peroxidation being an important mechanism of neurodegeneration in the AD brain. Aβ is widely reported to cause lipid peroxidation that is inhibited by antioxidants in brain cell membranes [4,12,52]. In addition, Aβ leads to 4-hydroxy-2-nonenal (HNE) and acrolein formation [33], and these alkenals alter the conformation of membrane proteins [45]. We have previously shown, consistently, an induction of HNE and 8-hydroxyguanosine (a marker of oxidative damage to DNA and RNA) immunoreactivities following infusion of Aβ (1–42) [21]. Protein oxidation is an important factor in aging and age-related neurodegenerative disorders [28,44]. Oxidative modification of proteins can lead to diminished functions for specific proteins [28,44]. Protein oxidation is most often indexed by the presence of protein carbonyls [44], which arise from a direct free radical attack on vulnerable amino acids side chains or from the products of glycation, glycoxidation, and lipid peroxidation reactions with protein (e.g., HNE and acrolein) [5]. The increased protein carbonyl in the AD brain, together with the altered activities of antioxidant enzymes (in some cases due to oxidation), coupled with studies showing that Aβ (1–42)- or Aβ (1–40)-induced neuronal protein oxidation can be inhibited by antioxidants [54], suggest that Aβ-induced protein oxidation may account, in part, for neurodegeneration in the AD brain.

α-Tocopherol is the most prevalent and efficacious lipid-soluble antioxidant in biological systems and inhibits the chain reaction of lipid peroxidation by trapping the chain carrying peroxyl radicals [38]. α-Tocopherol is reported to prevent the spatial learning deficit induced by i.c.v. injection of the cholinotoxin ethylcholine mustard aziridinium ion (AF64A), without affecting memory in control animals [49]. The ability of a number of antioxidants, including idebenone, α-tocopherol, and iron chelators, to abrogate GSH depletion-induced neurotoxicity [42] suggests that exogenously applied antioxidants are balancing the cellular antioxidant debt produced by GSH depletion. Furthermore, investigations in vitro have shown that α-tocopherol inhibits Aβ-induced neuronal cell death and protein oxidation [55], suggesting that oxidative stress is one of the mechanisms of the neurotoxicity of Aβ. Here, we confirmed that the imbalances in enzymatic antioxidants and the increases in lipid peroxidation and protein oxidation induced by Aβ (1–42) are prevented by α-tocopherol, confirming that oxidative stress is involved in at least part of the neurotoxic mechanism of the Aβ (1–42) in vivo.

Because elevated levels of copper, zinc, and iron are found in amyloid deposits of AD-affected brains [30], the oxidative stress observed in AD may be related to the production of reactive oxygen species by metal-bound forms of Aβ. Huang et al. [17] have shown that the binding of Cu^{2+} and Zn^{2+} to Aβ modulates the toxicity of the peptide through the generation of H_2O_2 by electron transfer to O_2. The binding of Cu^{2+} and Zn^{2+} to Aβ also induces the precipitation of the peptide [3,30]. Increased binding of these metals to Aβ is evident in AD [30], and it has been demonstrated that the metal-mediated redox activity and aggregation of Aβ, as well as amyloid deposition in APP 2576 transgenic mice, are inhibited by treatment with a bioavailable zinc/copper selective chelator, clioquinol [10]. Because α-tocopherol possesses metal chelating effects [9], we cannot rule out the possibility that the metal chelating effects of α-tocopherol may play a role in attenuating the imbalance of antioxidant enzymes and oxidative stress induced by Aβ (1–42) in mice.

Although Mn-SOD, in contrast to Cu,Zn-SOD, appeared to be not highly induced in the brain regions we examined, Aβ (1–42)-treated mice showed increased Mn-SOD activities at an early time point (2 days). This may be due to the formation of H_2O_2 in the mitochondria [7]. The relationship between mitochondrial damage, glutathione status/GSH dependent enzymes, oxidative stress, and neuronal dysfunction has been demonstrated by the effects of excessive production of H_2O_2 within mitochondria, which leads to depletion of mitochondrial GSH, in turn, causes the oxidation of protein thiols and the impairment of mitochondrial function [14]. Thus, it is possible that the loss of GSH may result in mitochondrial damage. It is likely that the converse situation is also true, namely, that impairment of mitochondrial function may lead to a decrease in cytosolic GSH. Because approximately 90% of total cellular GSH is localized in the cytosolic fraction [43], a GSH-depleted condition may be a common event leading to the disruption of the cellular activities of mitochondria and cytoplasm. GRX reduces oxidized GSSG back to two GSH molecules to replenish stores of this universal antioxidant. GSH and glutathione reductants, including GRX, have been shown to prevent mitochondrial oxidative damage [7]. However, GRX activity in this study was induced only at the early time-point after Aβ (1–42) treatment, suggesting that Aβ (1–42) might enhance mitochondrial toxicity in the brains of mice.

Cholinergic transmission is crucial to learning and memory, and its alteration is considered one of the main causes of cognitive disorder such as AD. As described in introduction, we have reported that Aβ (1–42 or 1–40) impairs cholinergic neuronal function, learning, and memory [18,39,40,46]. Similarly, a single i.c.v. injection of a picomolar dose of Aβ (1–42) effectively impaired learning and memory behaviour in mice. This behavioural abnormality was accompanied by decrease in cortical acetylcholine levels and increase in hippocampal glial fibrillary acidic protein (GFAP)-like immunoreactivity (GFAP-IR) [52], supporting previous reports in rats that continuous infusion of Aβ (1–40) blunts choline

acetyltransferase activity and increases GFAP-IR [39,40]. Further, Yan et al. [52] demonstrated that Aβ(1–42) injection induced a marked increase in interleukin-1β-like immunoreactivity (IL-1β-IR) in the hippocampus. Thus, in addition to the decreased acetylcholine levels, Aβ(1–42)-induced increase in IL-1β-IR may have contributed to learning and memory deficit in mice.

Interestingly, GSSG inhibits the binding of the specific ligand [^{3}H]quinuclidinyl benzilate to muscarinic cholinergic receptors [15], suggesting that GSH homeostasis is important in maintaining learning/memory functions [25]. We confirmed that α-tocopherol protects against Aβ-induced impaired homeostasis of GPX and GRX activities in this study. Thus, the present finding suggests that GSH-dependent antioxidant enzymes (GPX and GRX) are possible markers for evaluating antioxidant status, as well as learning/memory functions, of Aβ-treated model animals.

This study showed that a single i.c.v. injection of Aβ (1–42) resulted in significant impairment of memory function, imbalances in the activities of antioxidant enzymes, and increases in the oxidative stress (lipid peroxidation and protein oxidation) in mice, and that the potent antioxidant α-tocopherol significantly prevented these toxicities induced by Aβ (1–42). Therefore, our results suggest that oxidative stress contributes to Aβ (1–42)-induced learning and memory deficits in mice.

Acknowledgements

This study was supported by a grant of the Korea Health 21 R&D Project (02-PJ10-PG6-AG01-0003), Ministry of Health & Welfare, Republic of Korea.

References

[1] Aksenov MY, Tucker HM, Nair P, Aksenova MV, Butterfield DA, Estus S, et al. The expression of key oxidative stress-handling genes in different brain regions in Alzheimer's disease. J Mol Neurosci 1998;11:151–64.

[2] Behl C, Davis JB, Lesley R, Schubert D. Hydrogen peroxide mediates amyloid beta protein toxicity. Cell 1994;77:817–27.

[3] Bush AI, Pettingell WH, Multhaup G, Paradis MD, Vonsattel JP, Gusella JF, et al. Rapid induction of Alzheimer Aβ amyloid formation by zinc. Science 1994;265:1464–7.

[4] Butterfield DA, Hensley K, Harris M, Mattson M, Carney J. β-Amyloid peptide free radical fragments initiate synaptosomal lipoperoxidation in a sequence-specific fashion: implications to Alzheimer's disease. Biochem Biophys Res Commun 1994;200:710–5.

[5] Butterfield DA, Stadtman ER. Protein oxidation process in aging brain. Adv Cell Aging Gerontol 1997;2:161–91.

[6] Butterfield DA, Lauderback CM. Lipid peroxidation and protein oxidation in Alzheimer's disease brain: potential causes and consequences involving amyloid β-peptide-associated free radical oxidative stress. Free Radic Biol Med 2002;32:1050–60.

[7] Cassarino DS, Bennett Jr JP. An evaluation of the role of mitochondria in neurodegenerative diseases: mitochondrial mutations and oxidative pathology, protective nuclear responses, and cell death in neurodegeneration. Brain Res Rev 1999;29:1–25.

[8] Ceballos I, Nicole A, Briand P, Grimber G, Dalacourte A, Falment S, et al. Expression of human Cu–Zn superoxide dismutase gene in transgenic mice: model for gene dosage effect in Downs syndrome. Free Radical Res 1991;12/13:581–9.

[9] Cheng ZJ, Kuo SC, Chan SC, Ko FN, Teng CM. Antioxidant properties of butein isolated from *Dalbergia odorifera*. Biochim Biophys Acta 1998;1392:291–9.

[10] Cherny RA, Atwood CS, Xilinas ME, Gray DN, Jones WD, McLean CA, et al. Treatment with a copper–zinc chelator markedly and rapidly inhibits beta-amyloid accumulation in Alzheimer's disease transgenic mice. Neuron 2001;30:641–2.

[11] Coyle JT, Puttfarcken P. Oxidative stress, glutamate, and neurodegenerative disorders. Science 1993;262:689–95.

[12] Daniels WM, van Rensburg SJ, van Zyl JM, Taljaard JJ. Meltonin prevents beta-amyloid-induced lipid peroxidation. J Pineal Res 1998;24:78–82.

[13] Eklow L, Moldeus P, Orrenius S. Oxidation of glutathione during hydroperoxide metabolism. A study using isolated hepatocytes and the glutathione reductase inhibitor 1,3-bis(2-chloroethyl)-1-nitrosourea. Eur J Biochem 1984;138:459–63.

[14] Floyd RA, Carney JM. Free radical damage to protein and DNA: mechanisms involved and relevant observations on brain undergoing oxidative stress. Ann Neurol 1992;32:S22–S227.

[15] Frey WH, Najarian MM, Kurma KS, Emory CR, Menning PM, Frank JC, et al. Endogenous Alzheimer's brain factor and oxidized glutathione inhibit antagonist binding to muscarinic receptor. Brain Res 1996;724:87–94.

[16] Hendrie HC. Epidemiology of Alzheimer's disease. Geriatrics 1997;52:S4–8.

[17] Huang X, Atwood CS, Hartshorn MA, Multhaup G, Goldstein LE, Scarpa RC, et al. The Aβ peptide of Alzheimer's disease directly produces hydrogen peroxide through metal ion reduction. Biochemistry 1999;38:7609–16.

[18] Itoh A, Nitta A, Nodai M, Nishimura K, Hirose M, Hasegawa T, et al. Dysfunction of cholinergic and dopaminergic neuronal systems in β-amyloid protein-infused rats. J Neurochem 1996;66:1113–7.

[19] Itoh A, Akaike T, Sokabe M, Nitta A, Iida R, Olariu A, et al. Impairment of long-term potentiation in hippocampal slices of β-amyloid-infused rats. Eur J Pharmacol 1999;382:167–75.

[20] Jareno EJ, Bosch-Morell F, Fernandez-Delgado R, Donat J, Romero FJ. Serum malondialdehyde in HIV seropositive children. Free Radic Biol Med 1998;24:503–6.

[21] Jhoo WK, Kim HC, Yamada K, Im DH, Shin EJ, Park SJ, et al. Prolonged exposure to β-amyloid protein enhances 4-hydroxy-2-nonenal modifies proteins in the rat brain. Soc Neurosci Abstr 2000;26:1020.

[22] Kim HC, Jhoo WK, Choi DY, Im DH, Shin EJ, Suh JH, et al. Protection of methamphetamine nigrostriatal toxicity by dietary selenium. Brain Res 1999;851:76–86.

[23] Kim HC, Jhoo WK, Bing G, Shin EJ, Wie MB, Kim WK, et al. Phenidone prevents kainate-induced neurotoxicity via antioxidant mechanisms. Brain Res 2000;874:15–23.

[24] Kim HC, Bing G, Jhoo WK, Ko KH, Kim WK, Suh JH, et al. Changes of hippocampal Cu/Zn-superoxide dismutase after kainate treatment in the rat. Brain Res 2000;853:215–26.

[25] Kim HC, Yamada K, Nitta A, Olariu A, Tran MH, Mizuno M, et al. Immunocytochemical evidence that amyloid β (1–42) impairs endogenous antioxidant systems in vivo. Neuroscience 2003;119:399–419.

[26] Laursen SE, Belknap JK. Intracerebroventricular injections in mice. Some methodological refinements. J Pharmacol Meth 1986;16:355–7.

[27] Lawrence RA, Burk RF. Glutathione peroxidase activity in selenium-deficient rat liver. Biochem Biophys Res Commun 1976;71:952–8.

[28] Liu R, Liu IY, Thompson RF, Doctrow SR, Malfroy B, Baudry M. Reversal of age-related learning deficits and brain oxidative stress in

mice with superoxide dismutase/catalse mimics. Proc Natl Acad Sci USA 2003;100:8526–31.
[29] Lobo A, Launer LJ, Fratiglioni L, Andersen K, Di Carlo A, Breteler MM, et al. Prevalence of dementia and major subtypes in Europe: a collaborative study of population-based cohorts. Neurol Dis Elderly Res Group Neurol 2000;54:S4–9.
[30] Lynch T, Cherny RA, Bush AI. Oxidative processes in Alzheimer's disease: the role of Aβ-metal interactions. Exp Gerontol 2000;35:445–51.
[31] Lyras L, Cairns NJ, Jenner A, Jenner P, Halliwell B. An assessment of oxidative damage to proteins, lipids, and DNA in brain from patients with Alzheimer's disease. J Neurochem 1997;68: 2061–9.
[32] McCord JM, Fridovich I. Superoxide dismutase. Enzymatic function for erythrocuprein. J Biol Chem 1969;244:6049–55.
[33] Mark RJ, Lovell MA, Markesbery WR, Uchida K, Mattson MP. A role for 4-hydroxynonenal, an aldehydic product of lipid peroxidation, in disruption of iron homeostasis and neuronal death induced by amyloid β-peptide. J Neurochem 1997;68:255–64.
[34] Markesbery WR. Oxidative stress hypothesis in Alzheimer's disease. Free Radic Biol Med 1997;23:134–47.
[35] Matsuoka Y, Picciano M, La Francois J, Duff K. Fibrillar β-amyloid evokes oxidative damage in a transgenic mouse model of Alzheimer's disease. Neuroscience 2001;104:609–13.
[36] Maurice T, Lockhart BP, Privat A. Amnesia induced by centrally administered β-amyloid peptides involves cholinergic dysfunction. Brain Res 1996;706:181–93.
[37] Morris R. Developments of a water maze procedure for studying spatial learning in the rat. J Neurosci Meth 1984;11:47–60.
[38] Niki E, Yamamoto Y, Komuro E, Sato K. Membrane damage due to lipid peroxidation. Am J Clin Nutr 1991;53:201S–5S.
[39] Nitta A, Itoh A, Hasegawa T, Nabeshima T. β-Amyloid protein-induced Alzheimer's disease animal model. Neurosci Lett 1994;170:63–6.
[40] Nitta A, Fukuta T, Hasegawa T, Nabeshima T. Continous infusion of β-amyloid protein into cerebral ventricle induces learning impairment and neuronal and morphological degeneration. Jpn J Pharmacol 1997;73:51–7.
[41] Oliver CN, Ahn BW, Moerman EJ, Goldstein S, Statman ER. Age-related changes in oxidized proteins. J Biol Chem 1987;262:5488–91.
[42] Ratan RR, Murphy TH, Baraban JM. Macromolecular systhesis inhibitors prevent oxidative stress-induced apoptosis by shunting cystein to glutathione. J Neurosci 1994;14:4385–92.
[43] Reed DJ. Glutathione:toxicological implications. Ann Rev Pharmcol Toxicol 1990;30:603–31.
[44] Stadtman ER. Protein oxidation and aging. Science 1992;257: 1220–4.
[45] Subramaniam R, Roediger F, Jorda B, Mattson MP, Keller JN, Waeg G, et al. The lipid peroxidation product, 4-hydroxy-2-trans-nonenal, alters the conformation of cortical synaptosomal membrane proteins. J Nuerochem 1997;69:1161–9.
[46] Tran MH, Yamada K, Olariu A, Mizuno M, Ren XH, Nabeshima T. Amyloid β-peptide induces nitric oxide production in rat hippocampus: association with cholinergic dysfunction and amelioration by inducible nitric oxide synthase inhibitors. FASEB J 2001;15:1407–9.
[47] Tran MH, Yamada K, Nakajima A, Mizuno M, He J, Kamei H, et al. Tyrosine nitration of a synaptic protein synaptophysin contributes to amyloid β-peptide-induced cholinergic dysfunction. Mol Psychiatry 2003;8:407–12.
[48] Woo JI, Lee JH, Yoo KY, Kim CY, Kim YI, Shin YS. Prevalence estimation of dementia in a rural area of Korea. J Am Geriatr Soc 1998;46:983–7.
[49] Wortwein G, Stackman RW, Walsh TJ, Vitamin E. prevents the place learning deficit and the cholinergic hypofunction induced by AF64A. Exp Neurol 1994;125:15–21.
[50] Yamada K, Tanaka T, Zou LB, Senzaki K, Yano K, Osada T, et al. Long-term deprivation of oestrogens by ovariectomy potentiates β-amyloid-induced working memory deficits in rats. Br J Pharmacol 1999;128:419–27.
[51] Yamada K, Tanaka T, Han D, Senzaki K, Kameyama T, Nabeshima T. Protective effects of idebenone and alpha-tocopherol on β-amyloid-(1–42)-induced learning and memory deficits in rats: implication of oxidative stress in beta-amyloid-induced neurotoxicity in vivo. Eur J Neurosci 1999;11:83–90.
[52] Yan JJ, Cho JY, Kim HS, Kim KL, Jung JS, Huh SO, et al. Protection against beta-amyloid peptide toxicity in vivo with long-term administration of ferulic acid. Br J Pharmacol 2001;133:89–96.
[53] Yankner BA. Mechanisms of neuronal degeneration in Alzheimer's disease. Neuron 1996;250:279–82.
[54] Yatin SM, Varadarajan S, Link CD, Butterfield DA. In vitro and in vivo oxidative stress associated with Alzheimer's amyloid β-peptide (1–42). Neurobiol Aging 1999;20:325–30.
[55] Yatin SM, Varadarajan S, Butterfield DA. Vitamin E prevents Alzheimer's amyloid beta-peptide (1–42)-induced neuronal protein oxidation and reactive oxygen species production. J Alzheimers Dis 2000;2:123–31.

ELSEVIER

Journal of Neuroimmunology 163 (2005) 24–30

Journal of
Neuroimmunology

www.elsevier.com/locate/jneuroim

Mechanism of natural killer (NK) cell regulatory role in experimental autoimmune encephalomyelitis

Wen Xu[a,b], Gyorgy Fazekas[a], Hideo Hara[a,c], Takeshi Tabira[a,c,*]

[a]*Department of Demyelinating Disease and Aging, National Institute of Neuroscience, National Center of Neurology and Psychiatry, Kodaira, Ogawahigashi 4-1-1, Tokyo 187-8502, Japan*
[b]*Department of Immunology, Harbin Medical University, 157 BaoJian Road, Nan Gang District, Harbin 150086, People's Republic of China*
[c]*National Institute for Longevity Sciences, 36-3 Gengo, Morioka, Obu 474-8522, Japan*

Received 13 September 2004; received in revised form 2 February 2005; accepted 3 February 2005

Abstract

The mechanism of natural killer (NK) cell regulatory role in experimental autoimmune encephalomyelitis (EAE) was studied in SJL/J mice. In vivo experiments showed that NK cell depletion by anti-NK1.1 monoclonal antibody treatment enhanced EAE in mice. To investigate the mechanism, we cultured proteolipid protein $(PLP)_{136-150}$ peptide-specific, encephalitogenic T cell lines, which were used as the NK cell target. Our results show that NK cells exert a direct cytotoxic effect on autoantigen-specific, encephalitogenic T cells. Furthermore, cytotoxicity to PLP-specific, encephalitogenic T line cells was enhanced by using enriched NK cells as effector cells. However, the cytotoxic effect of NK cells to ovalbumin-specific T line cells and ConA-stimulated T cells could also be detected with a lesser efficiency. Our studies indicate that NK cells play a regulatory role in EAE through killing of syngeneic T cells which include myelin antigen-specific, encephalitogenic T cells, and thus ameliorate EAE.

Keywords: Natural killer cells; Experimental autoimmune encephalomyelitis; Proteolipid protein; Encephalitogenicity; Cytotoxicity

1. Introduction

Since the 1980s, a great deal of evidence has been accumulated, suggesting an association between decreased numbers and activities of NK cells and autoimmune diseases, such as multiple sclerosis (MS) (Benczur et al., 1980; Munschauer et al., 1995), type I diabetes (Nair et al., 1986; Negishi et al., 1986; Atallah et al., 1987), systemic lupus erythematosus (SLE) (Hoffman, 1980; Erkeller-Yuksel et al., 1993, 1997; Shai et al., 1999; Moser et al., 1998).

In multiple sclerosis (MS), it has been reported that MS patients tend to have lower numbers and activities of NK cells than healthy individuals and other neurological diseases patients (Vranes et al., 1989; Munschauer et al., 1995), and new and enlarging or recurring lesions tend to occur following periods of low NK cell activities (Kastrukoff et al., 1998). Although MS patients with stable symptoms had relatively normal lytic activities (Merrill et al., 1982; Neighbour et al., 1982), depressions in NK lytic activities immediately preceded lesion extension (Kastrukoff et al., 1998). It is interesting to know that the NK cell lytic activity of healthy monozygotic twin siblings of an affected patient was not changed (Kaudewitz et al., 1983; Heltberg et al., 1985).

In experimental autoimmune encephalomyelitis (EAE), a well-established model of MS, we have found that depletion of NK cells by in vivo treatment with a monoclonal antibody (mAb) against NK 1.1 resulted in an increased severity and relapsing pattern of disease in C57BL/6 mice (Zhang et al., 1997). It has also been reported that mAb (3.2.3 or anti-asialo GM1) depletion of NK cells exacerbates EAE in Lewis rats (Matsumoto et al., 1998).

* Corresponding author. National Institute for Longevity Sciences, 36-3 Gengo, Morioka, Obu 474-8522, Japan. Tel.: +81 562 45 0183; fax: +81 562 45 0184.
E-mail address: tabira@nils.go.jp (T. Tabira).

0165-5728/$ - see front matter © 2005 Elsevier B.V. All rights reserved.
doi:10.1016/j.jneuroim.2005.02.011

Although all of the evidence suggested that NK cells might play a role in the regulation of MS and EAE, the mechanism by which NK cells could mediate immune regulation remains unclear. The present study was conducted to investigate the mechanism of NK cell regulatory roles in EAE, and suggests direct killing of autoreactive T cells.

2. Materials and methods

2.1. Mice

SJL/J mice were purchased from Jackson Laboratory (Bar Harbor, ME). All mice were kept under specific pathogen-free conditions and only female mice (6–10 weeks old) were used. Experiments were conducted in accordance with our institutional guidelines after obtaining the permission of the Laboratory Animal Ethics Committee.

2.2. Reagents

$PLP_{136–150}$ (RVSHSLGKWLGHPDK) was purchased from Kurabo (Tokyo, Japan). Incomplete Freund's adjuvant (IFA) and heat-killed *Mycobacterium tuberculosis* H37Ra were purchased from Difco Laboratory (Detroit, MI). Pertussis toxin (PT), RPMI-1640, PKH 2, chicken OVA grade VII, and ConA were purchased from Sigma (St. Louis, MO). Hybridomas producing anti-NK1.1 mAb (PK136) and isotype-matched control mAb M-11, specific for human melanoma cell surface antigen, were obtained from American Type Culture Collection (Rockville, MD). The mAbs were purified from the supernatants using Protein A column chromatography. Anti-mouse CD_3-FITC, CD_{19}-PE, NK1.1-PE, DX_5-FITC and F_C Block (anti-mouse $F_C R\gamma$ II/III mAb) were purchased from PharMingen (San Diego, CA). Anti-mouse CD_{19} Microbeads and anti-mouse CD_5 Microbeads were purchased from Miltenyi Biotec (Bergisch Gladbach, Germany).

2.3. Immunization

For induction of active EAE, mice were injected in hind footpads with 200 μl of an emulsion containing 100 μg of $PLP_{136–150}$ in IFA supplemented with 400 μg of *M. tuberculosis*. Mice were injected intraperitoneally (i.p.) with 400 ng of pertussis toxin (PT) in 250 μl of phosphate-buffered saline (PBS) shortly after and 48 h after the immunization. For the study of T cell responses, mice were immunized only with the same emulsion without subsequent injection of PT.

2.4. EAE score

After immunization, mice were observed daily for clinical signs of EAE. The clinical grade was scored as follow: 0—no clinical signs; 1—loss of tail tonicity; 2—one hind leg paralysis; 3—two hind leg paralysis; 4—hind and fore leg paralysis; 5—death.

2.5. In vivo NK cell deletion

To deplete NK cells in vivo, mice were i.p. injected with 500 μg of anti-NK1.1 mAb (PK136) 1 day before and 14 days after the immunization. Control mice were treated either with 500 μg of an isotype-matched control mAb or PBS.

2.6. Quantitation of NK cells

Spleen cells were treated in ACK lysing buffer to lyse erythrocytes, washed three times in PBS, and then suspended in PBS containing 0.1% bovine serum albumin (BSA) and 0.01% NaN_3. The cells were first incubated with Fc Block (PharMingen, San Diego, CA) for 15 min to block nonspecific bindings of Ig to Fc receptors, washed in PBS, and then incubated with anti-CD_3-FITC, and/or anti-CD_{19}-PE, and/or anti-NK1.1 PE, and/or anti-DX_5-FITC for 30 min on ice. After washing, they were suspended in PBS containing 0.5 μg/ml of propidium iodide (PI; Wako Pure Chemical Industries, Ltd, Osaka, Japan), and 10,000 cells were analyzed by FACSort (Becton Dickinson, Mountain View, CA) with CellQuest software. Dead cells were excluded by gating out PI-positive cells.

2.7. Culture medium

RPMI-1640 containing 5×10^{-5} M 2-mercaptoethanol (2-ME), 2 mM L-glutamine, and 100 U/μg/ml penicillin/streptomycin (referred to as the basic medium) were used after supplemented with 10% or 5% fetal calf serum (FCS) alone or with 10% or 5% FCS and ConA supernatant as a source of IL-2 (supernatant of ConA-stimulated rat spleen cells).

2.8. T cell line culture

Long-term T cell lines specific for $PLP_{136–150}$ were established according to the method described (Inobe et al., 1993). Briefly, the draining lymph nodes were removed 10 days after immunization with $PLP_{136–150}$ and single cell suspensions were prepared at 5×10^6/ml in the basic medium supplemented with 10% FCS. They were plated on to 6-well plates at 5 ml/well and stimulated with 20 μg/ml $PLP_{136–150}$. The cells were fed with the basic medium supplemented with 10% ConA supernatant and 10% FCS every 3 days. On day 12, 5×10^5/ml T line cells were re-stimulated with 20 μg/ml $PLP_{136–150}$ in the presence of 5×10^6/ml X-irradiated (3300 rad), syngeneic spleen cells as APCs. After several cycles of alternate stimulation with $PLP_{136–150}$ and propagation (every 10–14 days), the antigen specificity and encephalitogenicity of the T cell lines were confirmed.

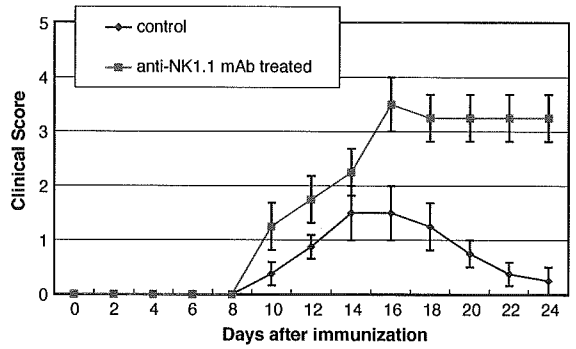

Fig. 1. NK cell depletion enhances EAE in SJL/J mice. Mice were immunized with 100 μg of $PLP_{136-150}$ in complete Freund adjuvant. Mice were also injected intraperitoneally with 400 ng of PT shortly after and 48 h after immunization. Anti-NK1.1 mAb-treated group mice were injected with 500 μg of anti-NK1.1 mAb (PK136) 1 day before and 14 days after immunization. Control mice were treated with PBS. Four mice in each group were used. This is a representative of three experiments with similar results.

OVA-specific T cell lines were established by using the same method.

2.9. ConA-stimulated T cell culture

Spleen cells from SJL/J mice were incubated on a plastic culture dish for 2–3 h at 37 °C, nonadherent cells were collected and incubated with CD_{19} Microbeads for 15 min at 6–12 °C, then T cells enriched population were negatively selected by passing through a MACS column.

1.25×10^6/ml T cells enriched population were cultured with 2.5 μg/ml ConA in RPMI-1640 supplemented with 5% FCS. The cultures were incubated for 72 h at 37°C in humidified air containing 5% CO_2, then cells were collected and used as target cells.

2.10. Cytotoxicity assay

Spleen cell suspensions were prepared from naïve SJL/J mice, and were treated with ACK buffer to lyse erythrocytes, then macrophages were depleted by adherence on a plastic culture dish for 2–3 h at 37 °C. Nonadherent cells were collected, washed with complete medium, and used as effector cells.

Cytotoxicity assays were performed using flow cytometric method of Slezak and Horan (Slezak and Horan, 1989). Briefly, 3 days after stimulation, cultured T line cells or ConA-stimulated T cells were labeled with a lipophilic green fluorescent cell linker PKH 2, which can incorporate into the cell membrane. Uniform labeling of cells was confirmed by visualization using a fluorescent microscope. Labeled target cells (*T*) were then incubated in triplicate with nonlabeled syngeneic effector cells (*E*) at ratio of 1:50, 1:100, 1:200, 1:400 (*T*:*E*) respectively for 4 h at 37 °C in humidified air containing 5% CO_2. Then cells were collected, stained with PI, and analyzed by flow cytometry. Controls consisted of cultured T line cells or ConA-stimulated T cells without effector cells. Cytotoxicity was determined by calculating the percentage of cells positive for both PI (red) and PKH 2 (green). NK cells cytotoxicity was expressed by subtracting the background from the average of three samples at each *E*:*T* ratio.

2.11. NK cells enrichment

Nonadherent spleen cells were prepared from naïve SJL/J mice as described above, then incubated with anti-mouse CD_{19} Microbeads and anti-mouse CD_5 Microbeads for 15 min at 6–12 °C. Then NK cells were negatively selected by passing through a MACS column according to the manufacturer's instructions. The purity of NK cells was examined by flow cytometry. Cytotoxicity assay was also performed by using enriched NK cells as effector cells.

2.12. Statistical analysis

Differences between groups were evaluated by student's *t* test. Statistical analysis was performed on the Excel program for Macintosh (Microsoft).

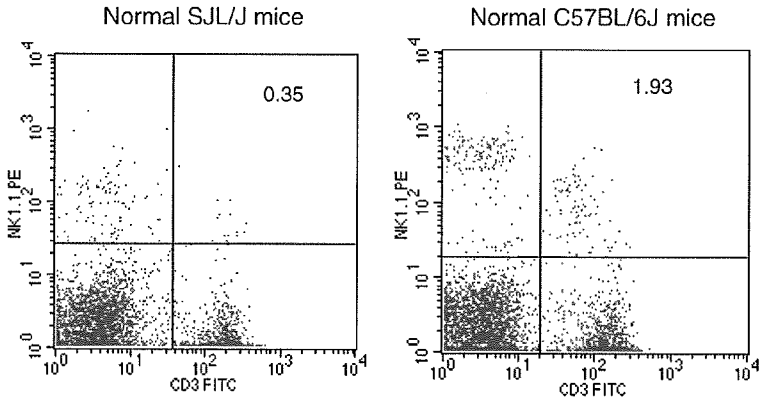

Fig. 2. Low NKT cell levels in SJL/J mice. Normal naive SJL/J mice and C57BL/6J mice spleen were removed, and stained with anti-NK1.1 PE and anti-CD3 FITC mAbs. One representative experiment out of three is shown.

3. Results

3.1. NK cell depletion enhanced EAE in SJL/J mice

3.1.1. In vivo NK cell depletion

Before and after treatment of naïve SJL/J mice with NK1.1 mAb, $CD_3^-NK1.1^+$ cells were 2.51%, 0.65%; $CD_{19}^-DX_5^+$ cells were 1.29%, 0.33%; and $DX_5^+NK1.1^+$ cells were 1.02%, 0.15% in the spleen, respectively. Thus, anti-NK1.1 mAb treatment depleted about 75% of NK cells in vivo.

Isotype-matched control mAb did not induce depletion of NK cells, which was proved both by previous work in our lab (Zhang et al., 1997) and by present work (data not show).

3.1.2. NK cell depletion enhanced EAE in SJL/J mice

Immunization with the used dose of $PLP_{136-150}$ induced a relatively mild form of EAE in untreated SJL/J mice and the mice injected with PBS. On the contrary, administration of anti-NK1.1 mAb 1 day before and 14 days after immunization resulted in aggravation of EAE, although the onset time of the two groups was not different discernibly. By the end of observation, the mice from the control group recovered almost completely, whereas the anti-NK1.1 mAb-treated mice did not show any recovery signs (Fig. 1). The clinical score of isotype-matched control mAb-treated mice was essentially the same as that of PBS-treated controls (data not show).

3.1.3. Low NKT cell levels in SJL/J mice

Anti-NK1.1 mAb depleted $NK1.1^+$ population which include both NK cells and NKT cells, NKT cells have also been suspected to be involved in the regulation of autoimmune processes (Mieza et al., 1996; Sumida et al., 1995; Fritz and Zhao, 2001). Interestingly, NKT cell population is quite low in SJL/J mice, much lower than that in C57BL/6J mice (Fig. 2).

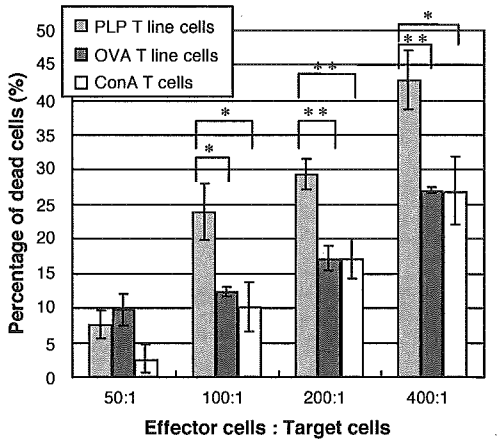

Fig. 4. Specificity of NK cell cytotoxicity. Cytotoxic effect of naïve mice splenic NK cells to PLP-specific T cell lines, OVA-specific T cell lines, and ConA-stimulated T cells were examined and compared by using the same method as described in the legend to Fig. 3. The final results were calculated by subtracting the background and expressed as mean ± S.E. of three samples at each *E*:*T* ratio. $^*P<0.05$; $^{**}P<0.01$.

3.2. NK cells exert direct cytotoxic effect on myelin antigen-specific, encephalitogenic T cells

The cultured PLP-specific, encephalitogenic T line cells were used as the target. The cytotoxicity of naïve mice splenic NK cells to the target was assayed by the flow cytometric method.

PKH 2-labeled cells showed a uniform mean fluorescence intensity of 10^2. If target cells were incubated alone without effector cells for 4 h, most of the target cells (94.38%) were still living (Fig. 3A). However, if the target cells were incubated with naïve mice spleen cells, after 4 h of incubation, the dead target cells, which were shown as PKH 2, PI double positive cells, increased obviously (Fig. 3B). Further more, the percentage of dead target cells

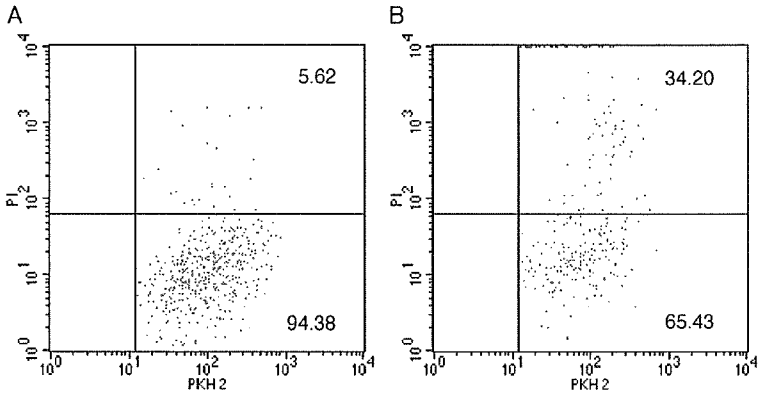

Fig. 3. NK cells exert direct cytotoxic effect on PLP-specific encephalitogenic T cell lines. The target T line cells were labeled with PKH 2, then labeled target cells were incubated with nonlabeled naïve mice spleen cells at the ratio of 50:1, 100:1, 200:1, 400:1 (Effector:Target). After 4 h of incubation, cells were harvested and stained with PI. Dead target T cells were double positive for both PKH 2 and PI, while living target cells were only positive for PKH 2. (A) without effector cells; (B) with effector cells at the ratio of 200:1. One representative experiment out of three is shown.

increased when the effector cells (SJL/J mice spleen cells) were increased in the culture in a dose-dependent manner (Figs. 4 and 6). This result implied that NK cells in the spleen exerted direct cytotoxic effect on PLP-specific, encephalitogenic target T cells.

3.3. Cytotoxicity to PLP-specific, encephalitogenic T line cells were enhanced by using enriched NK cells as effector cells

Before and after NK cell enrichment, $NK1.1^+$ cells were 3.99%, 29.19%; DX_5^+ cells were 2.38%, 30.56%; $NK1.1^+/DX_5^+$ cells were 1.93%, 25.97% respectively (Fig. 5).

Cytotoxicity to PLP-specific, encephalitogenic T line cells was enhanced by using enriched NK cells as effector cells (Fig. 6). This result further confirmed that the cytotoxicity to myelin antigen-specific T cells was due to the NK cells in the spleen.

3.4. NK cells also exert direct cytotoxic effect on OVA-specific T cell line and ConA-stimulated T cells

To investigate the specificity of NK cell cytotoxic effect on their targets, OVA-specific T cell line and ConA-stimulated T cells were also examined as target cells by exactly the same method as described above. We found that NK cells also exert direct cytotoxic effect on OVA-specific T line cells and ConA-stimulated T cells (Fig. 4). However, PLP-specific T line cells tended to be killed more efficiently.

4. Discussion

4.1. NK cells play a regulatory role in EAE

The present work demonstrated the inhibitory role of NK cells in EAE in SJL/J mice by in vivo treatment with

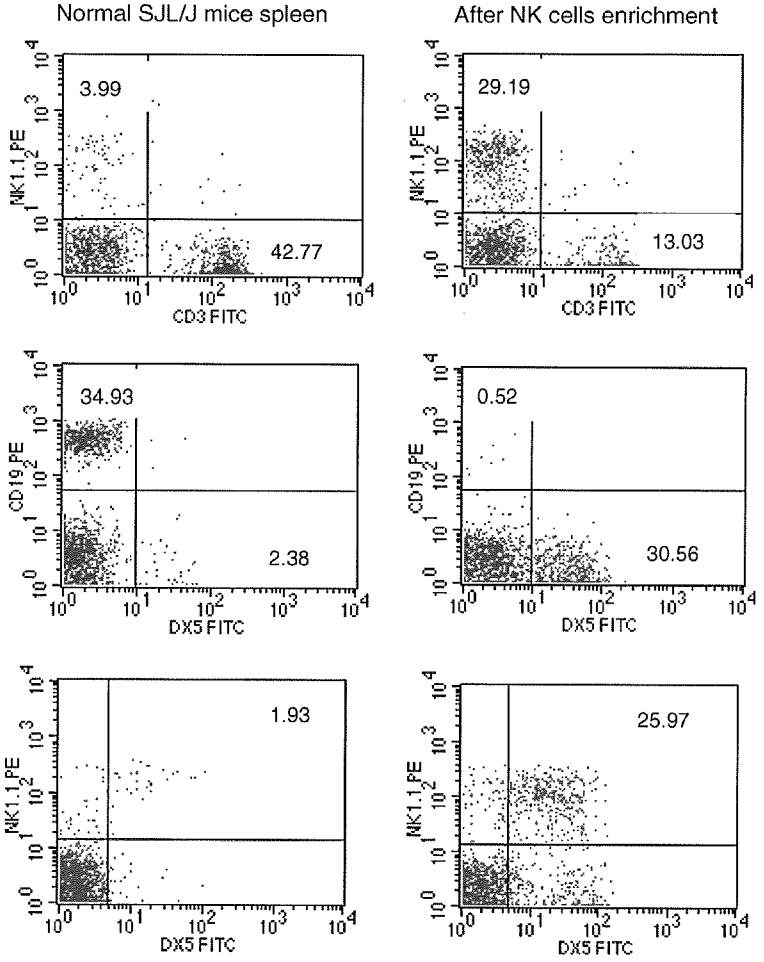

Fig. 5. NK cell enrichment. Nonadherent spleen cells which were prepared from naïve SJL/J mice were incubated with anti-mouse CD_{19} Microbeads and anti-mouse CD_5 Microbeads for 15 min. Then NK cells were negatively selected by passing through a MACS column. Then the purity of NK cells was examined and compared with that of normal SJL/J mice spleen cells.

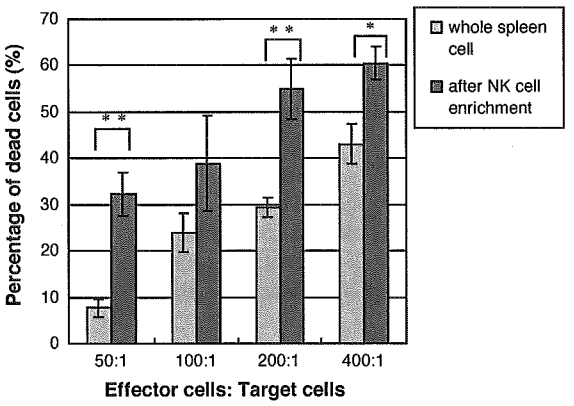

Fig. 6. Cytotoxicity to PLP-specific, encephalitogenic T line cells was enhanced by using enriched NK cells as effector cells. Cytotoxic effect to PLP-specific, encephalitogenic T cells by using naïve mice splenic NK cells and enriched NK cells as effector cells was examined and compared by using the same method as described in the legend to Fig. 3. The final results were calculated by subtracting the background and expressed as mean ± S.E. of three samples at each *E:T* ratio. $*P<0.05$; $**P<0.01$.

NK1.1 mAb (Fig. 1). Although we did not entirely exclude the involvement of NKT cells from the experiment, our previous paper shows that aggravation of EAE by NK cell deletion was also seen in β2-microglobulin$^{-/-}$ (β2m$^{-/-}$) mice, indicating that NK cells can play a regulatory role in a manner independent of CD8$^+$ T cells or NK1.1$^+$ T cells (NKT cells). Furthermore, EAE passively induced by the MOG $_{35-55}$-specific T cell line was also enhanced by NK cell deletion in B6, β2m$^{-/-}$, and recombination activation gene 2 (RAG-2)$^{-/-}$ mice, indicating that the regulation by NK cells can be independent of T, B, or NKT cells (Zhang et al., 1997). We found that the number of NKT cells is quite low in SJL/J mice, much lower than that of B6 mice (Fig. 2). Moreover, it has been reported that NKT cells in SJL/J mice are functionally deficient (Yoshimoto et al., 1995).

4.2. Mechanism of NK cell regulatory roles in EAE

What we are most interested in is the mechanism by which NK cells could mediate immune regulation. To date, the major effector activities of NK cells which have been identified are cytokine production and the ability of inducing target lysis. In our experiment, we proved the induction of target lysis by NK cells, although we cannot exclude that cytokines produced by NK cells also involved in the regulation of the disease. We found that NK cells exerted direct cytotoxic effect on newly stimulated myelin antigen-specific, encephalitogenic T cells, as well as OVA-specific T cells and ConA-stimulated T cells (Figs. 3 and 4). Although encephalitogenic T cells tended to be killed more efficiently, we conclude that NK cells play a regulatory role in EAE through killing of syngeneic T cells which include myelin antigen-specific, encephalitogenic T cells, thus ameliorate EAE. It has been reported that activated, but not resting T cells can be recognized and killed by syngeneic NK cells (Rabinovich et al., 2003), which may coincide with our observation. Although CD8$^+$ T cells could also exert cytotoxic effect on target cells, CD8$^+$ T cells are needed to be activated before they play their functional role. So we think it is unlikely that CD8$^+$ T cells could play an important role on cytotoxicity within 4 h of incubation. Furthermore, when using enriched NK cells in which CD_3^+ T cells were greatly decreased as effector cells (Fig. 5), we found that the cytotoxicity to myelin antigen-specific T cells were enhanced (Fig. 6). This result further indicated that NK cells in the spleen exerted cytotoxic effect on encephalitogenic T cells.

It has been known that NK cells induce target lysis via perforin (Kagi et al., 1994)- and/or TRAIL (Takeda et al., 2001)-dependent mechanisms. Although we have not yet examined the molecular mechanism of NK cell-mediated target lysis, it has been reported that blockade of TRAIL with its soluble receptor exacerbated EAE (Hilliard et al., 2001). We need to work further to identify the target molecule which may be expressed on the surface of the encephalitogenic T cells.

As to the therapy for MS, it has been accepted that type I interferon, especially IFN-β, is one of the standard therapy for relapsing–remitting and secondary progressive MS, and it is probably the most effective non-immunosuppressive therapy available now. And it is also well known that IFN-α/β increases cytotoxicity of NK cells. This is consistent with our conclusion that NK cells play a regulatory role in EAE through killing of syngeneic T cells which include myelin antigen-specific, encephalitogenic T cells, thus ameliorate EAE. Furthermore, on examining the effect of treating patients with relapsing–remitting MS with a high dose of IFN-β-1B, a strong inverse relationship between NK cell lytic activity and the number of active lesions identified by MRI was found in patients (Kastrukoff et al., 1999). It is interesting to know that TRAIL is a potential response marker for interferon-β treatment in multiple sclerosis (Wandinger et al., 2003). Other NK cell enhancer, such as Linomide, has also been reported to be able to suppress EAE (Karussis et al., 1993).

In summary, our results suggested that boosting NK cells in number and activity may be a promising immunotherapeutic strategy for multiple sclerosis and some other autoimmune diseases.

Acknowledgements

We thank Dr. Yoh Matsumoto for his valuable technique advice. We are also grateful to all of our colleagues for their helpful discussion throughout this work. This work was partially supported by the grant (Neuroimmunological Disorders) from the Ministry of Health, Labor, and Welfare, Japan.

References

Atallah, A.M., Abdelghaffar, H., Fawzy, A., Algharaoui, A., Alijani, M.R., Mahmoud, L.A., Ghoneim, M.A., Helfrich, G.B., 1987. Cell-mediated immunity and biological response modifiers in insulin-dependent diabetes mellitus complicated by end-stage renal disease. Int. Arch. Allergy Appl. Immunol. 83, 278–283.

Benczur, M., Petranyi, G.G., Palffy, G., Varga, M., Talas, M., Kotsy, B., Foldes, I., Hollan, S.R., 1980. Dysfunction of natural killer cells in multiple sclerosis: a possible pathogenic factor. Clin. Exp. Immunol. 39, 657–662.

Erkeller-Yuksel, F.M., Hulstart, F., Hannet, I., Isenberg, D., Lydyard, P., 1993. Lymphocyte subsets in a large cohort of patients with systemic lupus erythematosus. Lupus 2, 227–231.

Erkeller-Yuksel, F.M., Lydyard, P.M., Isenberg, D.A., 1997. Lack of NK cells in lupus patients with renal involvement. Lupus 6, 708–712.

Fritz, R.B., Zhao, M.L., 2001. Regulation of experimental autoimmune encephalomyelitis in the C57BL/6J mouse by NK1.1$^+$ DX5$^+$, $\alpha\beta^+$ T cells. J. Immunol. 166, 4209–4215.

Heltberg, A., Kalland, T., Kallen, B., Nilsson, O., 1985. A study of some immunological variables in twins discordant for multiple sclerosis. Eur. Neurol. 24, 361–373.

Hilliard, B., Wilmen, A., Seidel, C., Liu, T.-S.T., Goke, R., Chen, Y., 2001. Roles of TNF-related apoptosis-inducing ligand in experimental autoimmune encephalitis. J. Immunol. 166, 1314–1319.

Hoffman, T., 1980. Natural killer function in systemic lupus erythematosus. Arthritis Rheum. 23, 30–35.

Inobe, J.I., Yamamura, T., Kunishita, T., Tabira, T., 1993. T lymphocyte lines and clones selected against synthetic myelin basic protein 82–102 peptide from Japanese multiple sclerosis patients. J. Neuroimmunol. 46, 83–90.

Kagi, D., Ledermann, B., Burki, K., Seiler, P., Odermatt, B., Olsen, K.J., Podack, E.R., Zinkernagel, R.M., Hengartner, H., 1994. Cytotoxicity mediated by T cells and natural killer cells is greatly impaired in perforin-deficient mice. Nature 369, 31–37.

Karussis, D.M., Lehmann, D., Slavin, S., Vourka-karussis, U., Mizrachi-Koll, R., Ovadia, H., Ben-Nun, A., Kalland, T., Abramsky, O., 1993. Inhibition of acute experimental autoimmune encephalomyelitis by the synthetic immunomodulator Linomide. Ann. Neurol. 34, 654–660.

Kastrukoff, L.F., Morgan, N.G., Zecchini, D., White, R., Petkau, A.J., Satoh, J.-I., Paty, D.W., 1998. A role for natural killer cells in the immunopathogenesis of multiple sclerosis. J. Neuroimmnol. 86, 123–133.

Kastrukoff, L.F., Morgan, N.G., Zecchini, D., White, R., Petkau, A.J., Satoh, J., Paty, D.W., 1999. Natural killer cells in relapsing–remitting MS: effect of treatment with interferon beta-1B. Neurology 52, 351–359.

Kaudewitz, P., Zander, H., Abb, J., Ziegler-Heitbrock, H.W., Riethmuller, H.W., 1983. Genetic influence on natural cytotoxicity and interferon production in multiple sclerosis studies in monozygotic discordant twins. Hum. Immunol. 7, 51–58.

Matsumoto, Y., Kohyama, K., Aikawa, Y., Shin, T., Kawazoe, Y., Suzuki, Y., Tanuma, N., 1998. Role of natural killer cells and TCR$\gamma\delta$ T cells in acute autoimmune encephalomyelitis. Eur. J. Immunol. 28, 1681–1688.

Merrill, J., Jondal, M., Seely, J., Ullberg, M., Siden, A., 1982. Decreased NK killing in patients with multiple sclerosis: an analysis on the level of the single effecter cell in peripheral blood and cerebrospinal fluid in relation to the activity of disease. Clin. Exp. Immunol. 47, 419–430.

Mieza, M.A., Itoh, T., Cui, J.Q., Makino, Y., Kawano, T., Tsuchida, K., Koike, T., Shirai, T., Yagita, H., Matsuzawa, A., Koseki, H., Taniguchi, M., 1996. Selective reduction of V alpha 14+ NKT cells associated with disease development in autoimmune-prone mice. J. Immunol. 156, 4035–4040.

Moser, K.L., Neas, B.R., Salmon, J.E., Yu, H., Gray-McGuire, C., Asundi, N., Bruner, G.R., Fox, J., Kelly, J., Henshall, S., Bacino, D., Dietz, M., Houge, R., Koelsch, G., Nightingale, L., Shaver, T., Abdou, N.I., Albert, D.A., Carson, C., Petri, M., Treadwell, E.L., James, J.A., Hartley, J.B., 1998. Genome scan of human systemic lupus erythematosus: evidence for linkage on chromosome 1q in African–American pedigrees. Proc. Natl. Acad. Sci. U. S. A. 95, 14869–14874.

Munschauer, F.E., Hartrich, L.A., Stewart, C.C., Jacobs, L., 1995. Circulating natural killer cells but not cytotoxic T lymphocytes are reduced in patients with active relapsing multiple sclerosis and little clinical disability as compared to controls. J. Neuroimmunol. 62, 177–181.

Nair, M.P.N., Lewis, E.W., Schwartz, S.A., 1986. Immunoregulatory dysfunctions in type 1 diabetes: natural and antibody-dependent cellular cytotoxic activities. J. Clin. Immunol. 6, 363–372.

Negishi, K., Waldek, N., Buckingham, B., Kershnar, A., Fisher, L., Gupta, S., Charles, M.A., 1986. Natural killer and islet killer cell activities in type 1 (insulin dependent) diabetes. Diabetologia 29, 352–357.

Neighbour, P.A., Grayzel, A.I., Miller, A.E., 1982. Endogenous and interferon-augmented natural killer cell activity of human peripheral blood mononuclear cells in vitro. Studies of patients with multiple sclerosis, systemic lupus erythematosus and rheumatoid arthritis. Clin. Exp. Immunol. 49, 11–21.

Rabinovich, B.A., Li, J., Shannon, J., Hurren, R., Chalupny, J., Cosman, D., Miller, R.G., 2003. Activated, but not resting, T cells can be recognized and killed by syngeneic cells. J. Immunol. 170, 3572–3576.

Shai, R., Quismorio Jr., F.P., Li Jr., L., Kwon Jr., O.J., Morrison Jr., J., Wallace Jr., D.J., Neuwelt Jr., C.M., Braubar Jr., C., Gauderman Jr., W.J., Jacob Jr., C.O., 1999. Genome-wide screen for sysmetic lupus erythematosus susceptibility genes in multiple families. Hum. Mol. Genet. 8, 639–644.

Slezak, S.E., Horan, P.K., 1989. Cell-mediated cytotoxicity, a highly sensitive and informative flow cytometric assay. J. Immunol. Methods 177, 205–214.

Sumida, T., Sakamoto, A., Murata, H., Makino, Y., Takahashi, H., Yoshida, S., Nishioka, K., Iwamoto, I., Taniguchi, M., 1995. Selective reduction of T cells bearing invariant V alpha 24J alpha Q antigen receptor in patients with systemic sclerosis. J. Exp. Med. 182, 1163–1168.

Takeda, K., Hayakawa, Y., Smyth, M.J., Kayagaki, N., Yamaguchi, N., Kakuta, S., Iwakura, Y., Yagita, H., Okumura, K., 2001. Involvement of tumor necrosis factor-related apoptosis-inducing ligand in surveillance of tumor metastasis by liver natural killer cells. Nat. Med. 7, 94–100.

Vranes, Z., Poljakovic, Z., Marusic, M., 1989. Natural killer cell number and activity in multiple sclerosis. J. Neurol. Sci. 94, 115–123.

Wandinger, K.P., Lunemann, J.D., Wengert, O., Bellmann-Strobl, J., Aktas, O., Weber, A., Grundstrom, E., Ehrlich, S., Wernecke, K.D., Volk, H.D., Zipp, F., 2003. TNF-related apoptosis-inducing ligand (TRAIL) as a potential response marker for interferon-beta treatment in multiple sclerosis. Lancet 361, 2036–2043.

Yoshimoto, T., Bendelac, A., Li, J.H., Paul, W.E., 1995. Defective IgE production by SJL mice is linked to the absence of CD4$^+$, NK1.1$^+$ T cells that promptly produce interleukin 4. Proc. Natl. Acad. Sci. U. S. A. 92, 11931–11934.

Zhang, B., Yamamura, T., Kondo, T., Fujiwara, M., Tabira, T., 1997. Regulation of experimental autoimmune encephalomyelitis by natural killer (NK) cells. J. Exp. Med. 186, 1677–1687.

0026-895X/05/6806-1765–1774$20.00
MOLECULAR PHARMACOLOGY
Copyright © 2005 The American Society for Pharmacology and Experimental Therapeutics
Mol Pharmacol 68:1765–1774, 2005

Vol. 68, No. 6
11304/3064689
Printed in U.S.A.

Long-Lasting Impairment of Associative Learning Is Correlated with a Dysfunction of *N*-Methyl-D-aspartate–Extracellular Signaling-Regulated Kinase Signaling in Mice after Withdrawal from Repeated Administration of Phencyclidine

Takeshi Enomoto, Yukihiro Noda, Akihiro Mouri, Eun-Joo Shin, Dayong Wang, Rina Murai, Kazuo Hotta, Hiroshi Furukawa, Atsumi Nitta, Hyoung-Chun Kim, and Toshitaka Nabeshima

Department of Neuropsychopharmacology and Hospital Pharmacy, Nagoya University Graduate School of Medicine, Nagoya, Japan (T.E., Y.N., A.M., E.-J.S., D.W., R.M., K.H., A.N., T.N.); Division of Clinical Science in Clinical Pharmacy Practice, Management and Research, Faculty of Pharmacy, Meijo University, Nagoya, Japan (Y.N.); Neurotoxicology Program, College of Pharmacy, Kangwon National University, Chunchon, South Korea (E.-J.S., H.-C.K.); and Department of Medical Chemistry, Faculty of Pharmacy, Meijo University, Nagoya, Japan (H.F.)

Received January 21, 2005; accepted September 7, 2005

ABSTRACT

In humans, the administration of phencyclidine causes schizophrenic-like symptoms that persist for several weeks after withdrawal from phencyclidine use. We demonstrated here that mice pretreated with phencyclidine (10 mg/kg/day s.c. for 14 days) showed an enduring impairment of associative in a Pavlovian fear conditioning 8 days after cessation of phencyclidine treatment. Extracellular signaling-regulated kinase (ERK) was transiently activated in the amygdalae and hippocampi of saline-treated mice after conditioning. In the phencyclidine-treated mice, the basal level of ERK activation was elevated in the hippocampus, whereas the activation was impaired in the amygdala and hippocampus after conditioning. Exogenous *N*-methyl-D-aspartate (NMDA), glycine, and spermidine-induced ERK activation was not observed in slices of hippocampus and amygdala prepared from phencyclidine-treated mice. Repeated olanzapine (3 mg/kg/day p.o. for 7 days), but not haloperidol (1 mg/kg/day p.o. for 7 days), treatment reversed the impairment of associative learning and of fear conditioning-induced ERK activation in repeated phencyclidine-treated mice. Our findings suggest an involvement of abnormal ERK signaling via NMDA receptors in repeated phencyclidine treatment-induced cognitive dysfunction. Furthermore, our phencyclidine-treated mice would be a useful model for studying the effect of antipsychotics on cognitive dysfunction in schizophrenia.

In humans, phencyclidine, a noncompetitive *N*-methyl-D-aspartate (NMDA) receptor antagonist, has been shown to induce schizophrenia-like psychosis representing positive (e.g., hallucination and paranoia) and negative symptoms (e.g., emotional withdrawal and motor retardation) and cognitive dysfunction (Javitt and Zukin, 1991). It is interesting that such schizophrenia-like symptoms persisted for several weeks after withdrawal from long-term phencyclidine use (Rainey and Crowder, 1975; Allen and Young, 1978; Jentsch and Roth, 1999). Phencyclidine psychosis has been demonstrated to represent a drug-induced model of schizophrenia (Javitt and Zukin, 1991). We have reported previously that repeated phencyclidine treatment induces persistent enhancement of immobility in a forced swimming test (Noda et al., 1995, 2000) and social behavior deficit in mice (Qiao et al., 2001), which would be an animal model of negative symp-

This work was supported, in part, by grants-in-aid for scientific research from the Japan Society for the Promotion of Science (14370031, 15922139, 16922036, and 17390018), for Scientific Research on Priority Areas on "elucidation of glia-neuron network mediated information processing systems" from the Ministry of Education, Culture, Sports, Science and Technology (16047214), from a Funds from Integrated Molecular Medicine for Neuronal and Neoplastic Disorders (21st Century COE program), from the Japan Brain Foundation, from the Mitsubishi Pharma Research Foundation, and from an SRF Grant for Biomedical Research.

Article, publication date, and citation information can be found at http://molpharm.aspetjournals.org.
doi:10.1124/mol.105.011304.

ABBREVIATIONS: NMDA, *N*-methyl-D-aspartate; ERK, extracellular signaling-regulated kinase; NR1 subunit; *N*-methyl-D-aspartate receptor ζ subunit; MK-801, dizocilpine maleate; VEH, vehicle; OLZ, olanzapine; HAL, haloperidol; PCP, phencyclidine; ANOVA, analysis of variance; TBS, Tris-buffered saline; BDNF, brain-derived neurotrophic factor; PCP, phencyclidine.

toms. In cognitive function, it is well known that one-time administration of phencyclidine induces a transient cognitive dysfunction (Nabeshima et al., 1986; Noda et al., 2001). Jentsch and colleagues (1997a,b) have reported that repeated phencyclidine treatment induces an enduring working memory impairment in the T-maze of rats and memory impairment in an "object retrieval with a detour" task of monkeys. However, there were contradictory results about the enduring impairment of working memory in rats (Stefani and Moghaddam, 2002; Li et al., 2003). Although it has reported recently that spatial learning is impaired 1 day after repeated phencyclidine treatment in object recognition test of mice (Mandillo et al., 2003), it is not clear whether long-lasting cognitive dysfunction occurred in other types of learning and memory tasks.

Pavlovian fear conditioning is a useful tool for investigating associative learning, because the neuronal circuits underlying this task have been mapped (Maren, 2001). The cued fear conditioning depends on the amygdala, whereas the contextual fear conditioning depends on both the hippocampus and amygdala. Recent studies have identified the molecular basis of learning in this task. Activation of extracellular signaling-regulated kinase (ERK) via NMDA receptors in the hippocampus and amygdala is required for associative learning in fear conditioning (Atkins et al., 1998; Schafe et al., 2000; Athos et al., 2002).

The present study was designed to test the hypothesis that phencyclidine-pretreated mice develop an impairment of associative learning in Pavlovian fear conditioning after withdrawal from phencyclidine, and such impairment is mediated via a dysfunction of NMDA-ERK signaling. We attempted to investigate whether an impairment of associative learning is produced after repeated administration of phencyclidine and the changes of ERK activation in phencyclidine-treated mice after fear conditioning and NMDA receptor stimulation. Finally, for determining whether our model could be used as a model of the cognitive dysfunction in schizophrenia, the effects of haloperidol (a typical antipsychotic) and olanzapine (an atypical antipsychotic) on the associative learning in phencyclidine-treated mice were investigated.

Materials and Methods

Animals. Male mice of the ddY strain (Japan SLC Inc., Shizuoka, Japan), weighing 25 to 27 g at the beginning of experiments, were used. They were housed in plastic cages, received food (CE2; Clea Japan Inc., Tokyo, Japan) and water ad libitum, and were maintained on a 12/12-h light/dark cycle (lights on from 8:00 AM to 8:00 PM). All experiments were performed in accordance with the Guidelines for Animal Experiments of Nagoya University Graduate School of Medicine. The procedures involving animals and their care conformed to the international guidelines set out in the National Institutes of Health's *Guide for the Care and Use of Laboratory Animals.*

Cued and Contextual Fear Conditioning. Cued and contextual fear conditioning was performed according to a previous report (Nagai et al., 2003) with a minor modification. For measuring basal levels of freezing response (preconditioning phase), mice were individually placed in a neutral cage (17 × 27 × 12.5 cm) for 1 min and then in the conditioning cage (25 × 31 × 11 cm) for 2 min. For training (conditioning phase), mice were placed in the conditioning cage, and then a 15-s tone (80 dB) was delivered as a conditioned stimulus. During the last 5 s of the tone stimulus, a foot shock of 0.8 mA was delivered as an unconditioned stimulus through a shock generator (Neuroscience Idea Co. Ltd., Osaka, Japan). This procedure was repeated four times with 15-s intervals. Cued and contextual tests were carried out 1 to 2 h or 1 day after fear conditioning. For the cued test, the freezing response was measured in the neutral cage for 1 min in the presence of a continuous-tone stimulus identical with the conditioned stimulus. For the contextual test, mice were placed in the conditioning cage, and the freezing response was measured for 2 min in the absence of the conditioned stimulus.

Drugs. Phencyclidine HCl [1-(1-phenylcyclohexyl) piperidine hydrochloride] was synthesized by the authors according to the method of Maddox and colleagues (1965) and was checked for purity. Haloperidol (Sigma Chemical, St. Louis, MO) was purchased commercially. Olanzapine was supplied by Eli Lilly & Co. (Indianapolis, IN). Phencyclidine was dissolved in saline. Haloperidol and olanzapine were suspended in saline containing 0.1% (w/v) carboxymethyl cellulose sodium salt.

Drug Treatment. Phencyclidine (10 mg/kg/day s.c.) or saline was administered once a day for 14 consecutive days. Fear conditioning was performed 8 days after the withdrawal of repeated phencyclidine treatment. For investigating the effects of repeated antipsychotic treatment, mice were administered haloperidol (1 mg/kg/day p.o.), olanzapine (3 mg/kg/day p.o.), or vehicle once a day for 7 consecutive days from 1 day after the final phencyclidine treatment. On the day after the final haloperidol or olanzapine treatment, fear conditioning was performed. On the basis of our previous studies in a forced swimming test of mice (Noda et al., 1995, 2000), the doses of phencyclidine, olanzapine, and haloperidol were chosen. All compounds were administered in a volume of 0.1 ml/10 g body weight.

Western Blotting Analysis. Western blotting analysis was performed as described previously (Mizuno et al., 2002) with a minor modification. Before (basal) and immediately, 1 and 24 h after fear conditioning, the mice were killed by decapitation, and the brain was immediately removed. Hippocampi and amygdalae were rapidly dissected out, frozen, and stored at −80°C until used. The brain samples were homogenized in ice-cold buffer [50 mM Tris-HCl, pH 7.5, 150 mM NaCl, 10 mM NaF, 10 mM EDTA, 1% Nonidet P-40, 1 mM sodium orthovanadate, 10 mM sodium pyrophosphate, 0.5 mM dithiothreitol, 0.2 mM phenylmethylsulfonyl fluoride, 4 μg/ml pepstatin, 4 μg/ml aprotinin, and 4 μg/ml leupeptin for measuring ERK; or 20 mM Tris-HCl, pH 7.4, 150 mM NaCl, 50 mM NaF, 2 mM EDTA, 0.1% SDS, 1% sodium deoxycholate, 1% Nonidet P-40, 1 mM sodium orthovanadate, 20 μg/ml pepstatin, 20 μg/ml aprotinin, and 20 μg/ml leupeptin for measuring the NMDA receptor ζ subunit (NR1) and actin]. The lysate was centrifuged at 8000*g* for 10 min at 4°C. The protein concentration of the supernatant was determined by a Bradford assay (Bio-Rad, Hercules, CA). Sample buffer was added to the supernatant, and the mixture was boiled at 95°C for 5 min. Equivalent amounts of protein (50 μg) were electrophoresed on SDS-polyacrylamide gel, transferred to PVDF membranes (Millipore Corporation, Billerica, MA), and blocked with a Detector Block Kit (Kirkegaard and Perry Laboratories, Gaithersburg, MD). The membranes were incubated with anti-phospho-ERK antibody (1:1000; New England Biolabs, Beverly, MA), anti-NR1, CT antibody (1:1000; Upstate Biotechnology, Lake Placid, NY), or anti-actin antibody (C-11) (1:1000; Santa Cruz Biotechnology, Santa Cruz, CA) at 4°C overnight. The membranes were washed with the washing buffer (50 mM Tris-HCl, pH 7.4, 0.05% Tween 20, and 150 mM NaCl) three times for 10 min each. After incubation with secondary antibodies conjugated to horseradish peroxidase, the membranes were washed with the washing buffer three times for 10 min each. The immune complex was detected by an enhanced chemiluminescence kit (GE Healthcare, Little Chalfont, Buckinghamshire, UK) and exposed to X-ray film. Images on X-ray film were captured using charge-coupled device camera (Atto Bioscience, Tokyo, Japan). The band intensities were quantitatively analyzed using the Atto Densitograph Software Library Lane Analyzer. To measure total (phospho- and nonphospho-) ERK, membranes were stripped with stripping buffer (100 mM 2-melcaptoethanol, 2% SDS, and 62.5 mM Tris-HCl, pH 6.7) at 50°C for 10 min and incubated with anti-ERK antibody (1:1000; New

England Biolabs) at 4°C overnight. The immune complex was detected as described above. To evaluate the ERK activation, the phospho-ERK levels were normalized to the total ERK levels in the same membranes, and then each phospho-ERK/total ERK level was normalized to basal phospho-ERK/total ERK level in saline-treated mice. To evaluate the NR1 levels, the NR1 levels were normalized to the actin levels in the same membranes, and then each NR1/actin level was normalized to NR1/actin level in saline-treated mice.

Immunohistochemical Analysis. Immunohistochemical analysis was performed as described previously (Schafe et al., 2000; Kim et al., 2003) with a minor modification. Before and immediately after fear conditioning, mice were anesthetized with chloral hydrate (200 mg/kg i.p.) and then transcardially perfused with ice-cold 20 mM Tris-buffered saline (TBS) followed by 4% paraformaldehyde in 0.1 M Tris-HCl buffer, pH 7.4. Perfused brains were fixed at 4°C for 24 h in the same fixative and then immersed in 30% sucrose in TBS until the brain sank to the bottom. Immersed brains were cut into 30-μm transverse free-floating sections using a horizontal sliding microtome. For immunohistochemistry, sections were blocked in 0.3% hydrogen peroxide in TBS for 30 min and then followed by 30-min incubation in 0.4% Triton X-100, 4% normal goat serum, and 0.25% bovine serum albumin in TBS. After incubation in primary antibody against phospho-ERK (1:200) at 4°C for 48 h, sections were incubated in biotinylated anti-rabbit IgG (Vector Laboratories, Burlingame, CA) at room temperature for 2 h, and then followed by 1 h incubation in Avidin-Biotin complex (Vector Laboratories) at room temperature. 3-3′-Diaminobenzidine was used as a chromogen. According to a previous article (Sananbenesi et al., 2002), the density of phospho-ERK-stained cells were analyzed from the standardized area of 0.72 mm^2 in lateral and central amygdala, 1.58 to 1.70 mm posterior to bregma, using computer-based image analysis system (C. Imaging System; Compic, Mars, PA) attached to a light microscope (Olympus BX60-FLB-3; Olympus, Tokyo, Japan). To evaluate the ERK activation, the phospho-ERK levels after fear conditioning were normalized to the mean basal phospho-ERK level in each treatment.

Slice Stimulation. Slice stimulation was essentially preformed as described previously (Mamiya et al., 2003) with a minor modification. Eight days after the final phencyclidine treatment, the mice were killed by decapitation, and the brain was immediately removed. Amygdalae and hippocampi were dissected. Hippocampi were sliced at a thickness of 300 μm in a McIlwain tissue chopper (Mickle Laboratory Engineering, Gomshall, Surrey, UK). Amygdalae was sliced manually with a blade. After preincubation at 37°C in Ringer's buffer (10 mM HEPES-NaOH, pH 7.4, 135 mM NaCl, 5 mM KCl, 1 mM $CaCl_2$, 10 mM glucose; gassed with 95% O_2 and 5% CO_2) for 5 min, each slice was stimulated with NMDA (100 μM), glycine (10 μM), and spermidine (1 mM) for 5 min. After NMDA receptor stimulation, the slices were washed with ice-cold Ringer's buffer two times. The slices were homogenized as described above for Western blotting analysis.

Statistical Analysis. Statistical analysis was performed by one-way or two-way analysis of variance (ANOVA) using Bonferroni's test. The unpaired t test was used to compare two sets of data. A value of $p < 0.05$ was considered statistically significant. Data were expressed as the mean ± S.E.M.

Results

Effect of Repeated Phencyclidine Treatment on Fear Conditioning in Mice. In the preconditioning phase, both saline- and phencyclidine-treated mice hardly showed the freezing response. There were no differences in basal levels of freezing response between the two groups (data not shown). In cued (amygdala-dependent but hippocampus-independent) and contextual (amygdala- and hippocampus-dependent) fear conditioning, animals learned to fear tone and context associated with the room for foot shock. Both saline- and phencyclidine-treated mice showed marked cued and contextual freezing response 1 to 2 h after fear conditioning, and there was no significant difference between the two groups (Fig. 1, a and b). However, when cued and contextual freezing response was measured 1 day later, the phencyclidine-treated mice exhibited less freezing response (cued test: $p < 0.01$; contextual test: $p < 0.05$; Fig. 1, c and d). No alterations of nociceptive response were found in the phencyclidine-treated mice: the minimal current required to elicit flinching/running, jumping, or vocalization in the phencyclidine-treated mice was the same as that in the saline-treated mice (data not shown).

ERK Activation in the Amygdala and Hippocampus after Fear Conditioning. Phospho-ERK levels in the amygdala and hippocampus of the saline-treated mice were significantly increased immediately after fear conditioning, compared with basal levels (before conditioning) ($p < 0.01$, Fig. 2, a and b). The increase in phospho-ERK levels was transient and returned to basal levels within 1 h in both regions. In the amygdalae of the phencyclidine-treated mice, fear conditioning did not significantly increase the phospho-ERK levels compared with the basal level (Fig. 2a), and the phospho-ERK level immediately after conditioning in the phencyclidine-treated mice was significantly lower than that in the saline-treated mice ($p < 0.05$, Fig. 2a).

The basal phospho-ERK level in the hippocampi of the phencyclidine-treated unconditioned mice was significantly elevated compared with that in the saline-treated unconditioned mice ($p < 0.05$, Fig. 2b). However, fear conditioning did not cause a further increase compared with the basal level (Fig. 2b). Fear conditioning did not cause any changes in

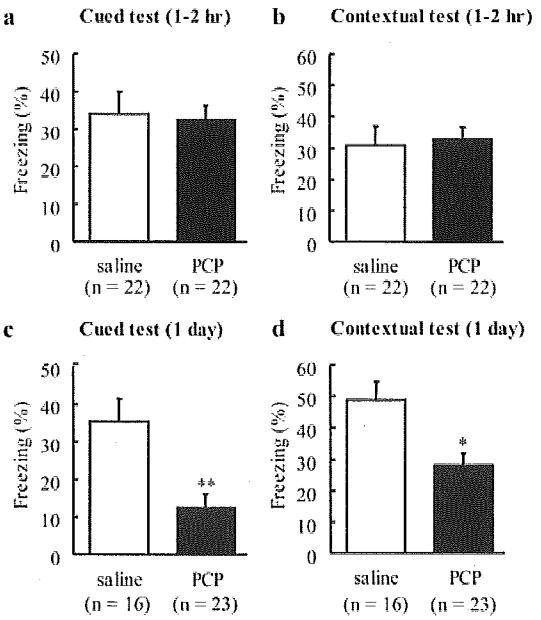

Fig. 1. Effect of repeated phencyclidine treatment on performance of fear conditioning in mice. Fear conditioning was performed 8 days after cessation of phencyclidine treatment (10 mg/kg/day s.c. for 14 days). Cued and contextual tests were performed 1 to 2 h (a, cued test; b, contextual test) and 1 day after fear conditioning (c, cued test; d, contextual test). Values correspond to mean ± S.E.M. *, $p < 0.05$ and **, $p < 0.01$ versus saline-treated mice (unpaired t test).